Inflammation-induced cholestasis in cancer cachexia

Morgane M Thibaut, Martina Sboarina, Martin Roumain, Sarah A Pötgens, Audrey M Neyrinck, Florence Destrée, Justine Gillard, Isabelle A Leclercq, Guillaume Dachy, Jean-baptiste Demoulin, et al.

ORIGINAL ARTICLE

Journal of Cachexia, Sarcopenia and Muscle 2021; **12**: 70–90
Published online 22 December 2020 in Wiley Online Library (wileyonlinelibrary.com) **DOI:** 10.1002/jcsm.12652

Inflammation-induced cholestasis in cancer cachexia

Morgane M. Thibaut[1], Martina Sboarina[1], Martin Roumain[2], Sarah A. Pötgens[1], Audrey M. Neyrinck[1], Florence Destrée[1], Justine Gillard[3], Isabelle A. Leclercq[3], Guillaume Dachy[4], Jean-Baptiste Demoulin[4], Anne Tailleux[5], Sophie Lestavel[5], Marialetizia Rastelli[1,6], Amandine Everard[1,6], Patrice D. Cani[1,6], Paolo E. Porporato[7], Audrey Loumaye[8], Jean-Paul Thissen[8], Giulio G. Muccioli[2], Nathalie M. Delzenne[1] & Laure B. Bindels[1]*

[1]*Metabolism and Nutrition Research Group, Louvain Drug Research Institute, UCLouvain, Université catholique de Louvain, Brussels, Belgium,* [2]*Bioanalysis and Pharmacology of Bioactive Lipids Research Group, Louvain Drug Research Institute, UCLouvain, Université catholique de Louvain, Brussels, Belgium,* [3]*Laboratory of Hepato-Gastroenterology, Institut de Recherche Expérimentale et Clinique, UCLouvain, Université catholique de Louvain, Brussels, Belgium,* [4]*Experimental Medicine Unit, de Duve Institute, UCLouvain, Université catholique de Louvain, Brussels, Belgium,* [5]*Université de Lille, Inserm, CHU Lille, Institut Pasteur de Lille, U1011-EGID, Lille, France,* [6]*Walloon Excellence in Life Sciences and BIOtechnology (WELBIO), Louvain Drug Research Institute, UCLouvain, Université catholique de Louvain, Brussels, Belgium,* [7]*Department of Molecular Biotechnology and Health Science, Molecular Biotechnology Center, University of Turin, Turin, Italy,* [8]*Endocrinology, Diabetology and Nutrition Department, Institut de Recherche Expérimentale et Clinique, UCLouvain, Université catholique de Louvain, Cliniques Universitaires Saint-Luc, Brussels, Belgium*

Abstract

Background Cancer cachexia is a debilitating metabolic syndrome contributing to cancer death. Organs other than the muscle may contribute to the pathogenesis of cancer cachexia. This work explores new mechanisms underlying hepatic alterations in cancer cachexia.

Methods We used transcriptomics to reveal the hepatic gene expression profile in the colon carcinoma 26 cachectic mouse model. We performed bile acid, tissue mRNA, histological, biochemical, and western blot analyses. Two interventional studies were performed using a neutralizing interleukin 6 antibody and a bile acid sequestrant, cholestyramine. Our findings were evaluated in a cohort of 94 colorectal cancer patients with or without cachexia (43/51).

Results In colon carcinoma 26 cachectic mice, we discovered alterations in five inflammatory pathways as well as in other pathways, including bile acid metabolism, fatty acid metabolism, and xenobiotic metabolism (normalized enrichment scores of −1.97, −2.16, and −1.34, respectively; all *P*adj < 0.05). The hepatobiliary transport system was deeply impaired in cachectic mice, leading to increased systemic and hepatic bile acid levels (+1512 ± 511.6 pmol/mg, $P = 0.01$) and increased hepatic inflammatory cytokines and neutrophil recruitment to the liver of cachectic mice (+43.36 ± 16.01 neutrophils per square millimetre, $P = 0.001$). Adaptive mechanisms were set up to counteract this bile acid accumulation by repressing bile acid synthesis and by enhancing alternative routes of basolateral bile acid efflux. Targeting bile acids using cholestyramine reduced hepatic inflammation, without affecting the hepatobiliary transporters (e.g. tumour necrosis factor α signalling via NFκB and inflammatory response pathways, normalized enrichment scores of −1.44 and −1.36, all *P*adj < 0.05). Reducing interleukin 6 levels counteracted the change in expression of genes involved in the hepatobiliary transport, bile acid synthesis, and inflammation. Serum bile acid levels were increased in cachectic vs. non-cachectic cancer patients (e.g. total bile acids, +5.409 ± 1.834 μM, $P = 0.026$) and were strongly correlated to systemic inflammation (taurochenodeoxycholic acid and C-reactive protein: $\rho = 0.36$, *P*adj = 0.017).

Conclusions We show alterations in bile acid metabolism and hepatobiliary secretion in cancer cachexia. In this context, we demonstrate the contribution of systemic inflammation to the impairment of the hepatobiliary transport system and the role played by bile acids in the hepatic inflammation. This work paves the way to a better understanding of the role of the liver in cancer cachexia.

Keywords Liver; Hepatobiliary transport system; Bile acids; IL-6; Cholestyramine

Received: 28 May 2020; Revised: 22 September 2020; Accepted: 2 November 2020
**Correspondence to: Laure B. Bindels, Metabolism and Nutrition Research Group, Louvain Drug Research Institute, UCLouvain, Université catholique de Louvain, Avenue E. Mounier, 73, B1.73.11, Brussels, Belgium. Email: laure.bindels@uclouvain.be*

Introductory statement

Cancer cachexia is a multifactorial syndrome characterized by body weight loss, weakness, muscle atrophy, fat depletion, thermogenesis, and systemic inflammation.[1–4] It affects up to 70% of cancer patients, depending on cancer types, and is responsible for at least 22% of cancer deaths.[1,5,6] Cancer cachexia does result not only in increased mortality rates but also in increased morbidity and reduced tolerance to anti-cancer treatments.[7] Cancer cachexia is a multi-organ syndrome driven, among other factors, by systemic inflammation and altered hormone production. Several pro-inflammatory mediators and tumour-derived catabolic factors are generated through a tumour-immune crosstalk and have been shown to drive communication between the tissues such as tumour, muscle, adipose tissue, and liver.[1,2,8]

Although often overlooked, alterations in liver metabolism could widely contribute to the increased energy dissipation and should also be considered to understand the pathogenesis of cancer cachexia. In cancer patients, modelling energy cost showed that hepatic futile cycles represent a large proportion of the whole-body energy demand.[9,10] In addition, the activation of the liver acute phase response was observed in cancer cachexia and has been correlated with increased resting energy expenditure in pancreatic cancer patients.[11] It has also been proposed that the liver acute phase response can lead to unbalanced amino acid composition and significantly contribute to muscle atrophy in these patients.[12] Beside this, a few changes in the liver metabolism have been reported in rat and mouse models of cachexia. These changes ranged from alterations in mitochondrial function and decreased oxidative phosphorylation[13–15] to increased hepatic triglyceride levels leading to hepatic steatosis,[16,17] and hepatic collagen deposition and fibrosis.[18] However, understanding how liver dysfunction contributes to cancer cachexia development still remains to be explored, and further investigations are required to fully harness the liver as a target in the treatment of cancer-associated cachexia.

Cancer cachexia is largely characterized by systemic inflammation, including increased pro-inflammatory cytokines such as interleukin 1 (IL-1), interleukin 6 (IL-6), and tumour necrosis factor α (TNFα).[19,20] Furthermore, it is generally accepted that inflammatory mediators affect the hepatobiliary transport system by a process termed as 'inflammation-induced cholestasis'. The latter is observed in several conditions including, among others, viral or drug-induced hepatitis and systemic or extrahepatic bacterial infections.[21,22] Common mediators of this process are endotoxins [mainly lipopolysaccharides (LPS)] that can reach the liver, leading to the production of local inflammatory cytokines, mainly by Kupffer cells. These cytokines, through the activation of signalling pathways in hepatocytes and cholangiocytes, may alter the expression and function of bile acid transporters inducing an accumulation of bile acids in the liver.[22–24] At this point, compensatory adaptive responses occur through nuclear receptors at multiple levels to avoid the accumulation of potentially toxic biliary components. Consequently, several changes take place including a down-regulation of bile acid synthesis, down-regulation of phase I and II detoxification enzymes, as well as up-regulation of alternative bile acid secretion efflux.[25,26] In case bile acids do still accumulate despite these adaptations, cholestatic hepatocytes may induce the expression of pro-inflammatory mediators leading to neutrophil accumulation and liver injury.[27–29]

Cholestasis has been described in a few specific cases of paraneoplastic conditions. Impairment of bile secretion appeared in Stauffer's syndrome, a rare complication occurring in patients with renal carcinoma, and in a limited number of case reports in paraneoplastic conditions in Hodgkin's lymphoma and prostate carcinoma.[30–32] In the context of cancer-associated cachexia, alterations in bile secretion could exacerbate hepatic inflammation because of increased levels of toxic circulating bile acids and could also affect lipid digestion and participate to intestinal malabsorption. Interestingly, treatment with ursodeoxycholic acid (UDCA), a bile acid with anti-inflammatory and anti-apoptotic properties, showed a trend towards attenuation of tissue loss in the Yoshida hepatoma model.[33] However, the hypothesis of an implication of bile acids in hepatic and systemic alterations associated with cancer progression has never been investigated so far. Such investigation may lead to a better understanding of the contribution of the liver to cancer cachexia.

In the present work, we analysed the hepatic whole transcriptome of cachectic mice bearing ectopic tumour to identify new pathways affected by the disease. Along with the activation of classical inflammatory pathways, we discovered that bile acid and xenobiotic metabolism pathways are some of the most deeply down-regulated ones. These observations, in line with our current knowledge of inflammation-induced cholestasis, led us to hypothesize that the hepatobiliary transport system is disturbed in cancer cachexia.

Experimental procedure

Cell culture

Colon carcinoma 26 (C26) and Lewis lung carcinoma (LLC) cells were maintained in Dulbecco's Modified Eagle Medium high-glucose medium supplemented with 10% foetal bovine serum (PAA clone, PAA, Austria), 100 μg/mL streptomycin and 100 IU/mL penicillin (Thermo Fisher, Belgium) at 37°C with 5% CO_2.

Mouse experiments

Male CD2F1 mice (7 weeks old, Charles River Laboratories, Italy) were kept in specific pathogen-free conditions and housed in individually ventilated cages with a 12 h light/dark cycle and fed an irradiated chow diet (AO4-10, Safe, France). After 1 week acclimatization, either a saline solution or C26 cells (1×10^6 cells in 0.1 mL saline) were subcutaneously injected. Food intake and body weight were recorded. Eight mice were randomly assigned in each group based on their body weight on the day of cell injection. When appropriate, mice received cholestyramine (Sigma-Aldrich, MO, USA) at 2% w/w in their diet, from Day 1 after cell injection until the end of the experiment. Ten days after cancer cell injection, mice were fasted from 7 a.m. to 1 p.m., and tissue samples were harvested following anaesthesia (isoflurane gas, Abbot, Belgium). Tissues were weighed and frozen in liquid nitrogen, with hepatic sections stored in 4% paraformaldehyde and embedded in paraffin. All samples were stored at −80°C until further analyses. Experiments regarding the administration of a neutralizing IL-6 antibody, the pair-feeding, and the kinetic assessment are described in the Supporting Information, *Data* S1.

All the experiments performed in Belgium were approved by and performed in accordance with the guidelines of the local ethics committee from the UCLouvain, Belgium. Housing conditions were as specified by the Belgian Law of 29 May 2013, regarding the protection of laboratory animals.

For the LLC model, C57Bl/6J mice (local husbandry, Torino, Italy) were kept in specific pathogen-free conditions and housed in individually ventilated cages with a 12 h light/dark cycle and fed an irradiated standard chow diet. LLC cells were injected in the right bottom flank at 1×10^6 cells in 0.1 mL saline and mice were necropsied 21 days after cell injection. The experiment was performed in accordance with local and national committees based on Italian Law DL 26/2014.

Hepatic whole transcriptome

Hepatic RNA samples were sequenced after polyA selection using a 2 × 150 paired end (PE) configuration on an Illumina HiSeq 4000 instrument (Genewiz, Germany). Raw sequence data generated from Illumina HiSeq were processed using Illumina's bcl2fastq 2.17 software. Raw fastq files were analysed in house using well-established bioinformatic pipeline, described in the Supporting Information, *Data* S1. The RNA sequencing dataset generated and analysed for this study can be found in Gene Expression Omnibus (GSE154219).

Bile acid quantification

Bile acid quantification was performed by high-performance liquid chromatography–mass spectrometry following a previously described approach.[34] The detailed procedure can be found in the Supporting Information, *Data* S1.

Tissue mRNA analysis

Total RNA was isolated from tissue by TriPure reagent (Roche, Basel, Switzerland). cDNA was prepared by reverse transcription of 1 μg total RNA using the Reverse Transcription System or the GoScript RT Mix Oligo(dT) kit (Promega, Leiden, The Netherlands). Real-time polymerase chain reactions (PCRs) were performed with a StepOnePlus/QuantStudio real-time PCR system and software (Applied Biosystems, Den Ijssel, The Netherlands) or a CFX96 Touch™ instrument and software (Bio-Rad Laboratories, CA, USA) using SYBR Green (Applied Biosystems, Promega, or Eurogentec, Seraing, Belgium) for detection. All samples were run in duplicate in a single 96-well reaction plate, and data were analysed according to the $2^{-\Delta\Delta CT}$ method. The purity of the amplified product was verified by analysing the melt curve performed at the end of amplification. The ribosomal protein L19 (*Rpl19*) gene or the ribosomal protein L6 (*Rpl6*) gene was used as housekeeping gene, at the exception of the brown adipose tissue where the ornithine decarboxylase antizyme 1 (*Oaz1*) was selected as housekeeping gene. The primer sequences for the targeted mouse genes are detailed in the Supporting Information, *Table* S1.

Histological, western blot, and biochemical analyses

Immunohistochemistry was performed on paraffined sections obtained from a fraction of the main liver lobe. Briefly, the sections were dewaxed using decreasing concentrations of isopropanol. Endogenous peroxidases were inhibited using a solution containing methanol and H_2O_2 3%, and the antigen retrieval was performed in EDTA buffer (pH 8, 95°C for 30 min). Labelling was performed using Ly-6G rat anti-mouse (BD Pharmingen, 551459) diluted 1:2000 for primary antibody, rabbit anti-rat (Vector, AI-4001) diluted 1:100 for secondary antibody, Envision anti-rabbit-HRP (Dako, K4003) and DAB (Dako, K3468). Haematoxylin was used for counterstaining. Sections were digitalized at a 20× magnification using a SCN400 slide scanner (Leica, Wetzlar, Germany). The quantification of number of neutrophils per square millimetre was determined by a blind procedure using the software TissueIA (version 4.0.7). Haematoxylin and eosin-stained sections were digitalized at a 20 × magnification using the same scanner.

Total bilirubin quantification was performed using the Bilirubin Assay kit (Sigma-Aldrich, MAK126). Alanine aminotransferase (ALAT) quantification was performed following the protocol provided by DiaSys Diagnostic System [ALAT (GPT) FS]. The alkaline phosphatase activity was determined by the measurement of the formation of *p*-nitrophenol from *p*-nitrophenylphosphate, with *p*-nitrophenol as standard (both from Sigma-Aldrich), based on the protocol of Bessey *et al*.[35]

The detailed procedure of western blot analyses can be found in the Supporting Information, *Data* S1.

Cross-sectional prospective study with cancer patients

The cohort of patients and its characterization were previously reported.[36,37] This cross-sectional prospective study was performed at the *Cliniques universitaires Saint-Luc*, Brussels, Belgium. The protocol was approved by the ethics committee of the UCLouvain (NCT01604642).

Patients with colorectal cancer, confirmed by anatomopathology, were recruited at the diagnosis or at relapse, before any therapeutic intervention, from January 2012 to March 2014. Written consent was given prior to entry into the study. Exclusion criteria were: non-Caucasian subjects, obvious malabsorption, major depression, artificial nutrition, high doses of steroids ($>$1 mg/kg hydrocortisone equivalent), hyperthyroidism, other causes of malnutrition, major walking handicap, Eastern Cooperative Oncology Group performance status $\geq$4 and psychological, familial, social, or geographic conditions that would preclude participation in the full protocol. The cachectic status was determined according to the definition proposed by Fearon *et al*., as an involuntary weight loss $>$5% over the past 6 months or weight loss $>$2% and body mass index $<$20 kg/m^2 or weight loss $>$2% and low muscularity. Additional information is provided in the Supporting Information, *Data* S1 and *Table* S5.

Statistical analyses

Data were analysed using a Student *t*-test when comparing two groups, one-way ANOVA followed by Dunnett's pairwise comparison post-hoc tests with the C26 group as reference for the cholestyramine study, or one-way ANOVA with Tukey's post-hoc tests for the neutralizing IL-6 antibody study. All data were checked for normality using the Shapiro–Wilk normality test. Data determined to be non-normal even after log-transformation were analysed using a Mann–Whitney U-test or Kruskal–Wallis test with Dunn's post-tests. Outliers were removed using the Grub's test. Statistical analyses were carried out using GraphPad Prism 5.0 (GraphPad Software, San Diego, CA, USA) and R. $P < 0.05$ was considered statistically significant.

Correlation analyses were performed in R using Pearson correlations for the mouse kinetic experiment (R package *Hmisc*) and partial Spearman correlations for the clinical study (*pcor* function, http://www.yilab.gatech.edu/pcor.html, correction for age and sex). An adjusted *P* value was computed to account for multiple testing using the Benjamini and Hochberg procedure. Heat maps were generated using the R package *gplots*.

Results

Pathways including inflammation, bile acid metabolism, and xenobiotic metabolism are altered in the liver of C26 cachectic mice

The C26 cachexia model is a well-established model of cachexia characterized by a relatively small tumour mass, with decreased food intake and loss of body weight due to muscle and adipose tissue wasting.[38] To identify hepatic disturbances associated with cancer cachexia, a hepatic whole transcriptome analysis was performed for cachectic mice (C26 mice) and sham-injected mice (CT mice) (eight mice per group). Exploratory multivariate analysis of the 22 389 genes expressed in the liver of these mice showed a clear distinction between control and cachectic mice (*Figure* 1A). Our univariate analysis highlighted 1844 significantly up-regulated and 1712 significantly repressed genes in cachectic mice [*P*adj $<$ 0.01, absolute $\log_2$(fold-change) $>$1] (full list in the Supporting Information, *Table* S2). Volcano plot of differentially expressed hepatic genes between control mice and cachectic mice clearly showed that *Oatp2* (*Sclo1a4*), a bile acid transporter, and *Ugt2b1*, a phase II drug-metabolizing enzyme, were two major down-regulated genes and that many genes involved in the inflammatory response were induced (*Figure* 1B). To identify the function of the altered genes, we performed a gene set enrichment analysis that revealed an up-regulation of genes implicated in IL-6/JAK/STAT-3 signalling, coagulation, epithelial mesenchymal transition, TNFα signalling via NFκB, complement, unfolded protein response, and inflammatory response (*Figure* 1C). Conversely, the main down-regulated pathways were oxidative phosphorylation, fatty acid metabolism, and bile acid metabolism (including genes such as *Cyp8b1* and *Cyp7a1*), as well as xenobiotic metabolism (including genes such as *Cyp1a1* and *Cyp1a2*) (*Figure* 1C, full list of leading genes in the Supporting Information, *Table* S3).

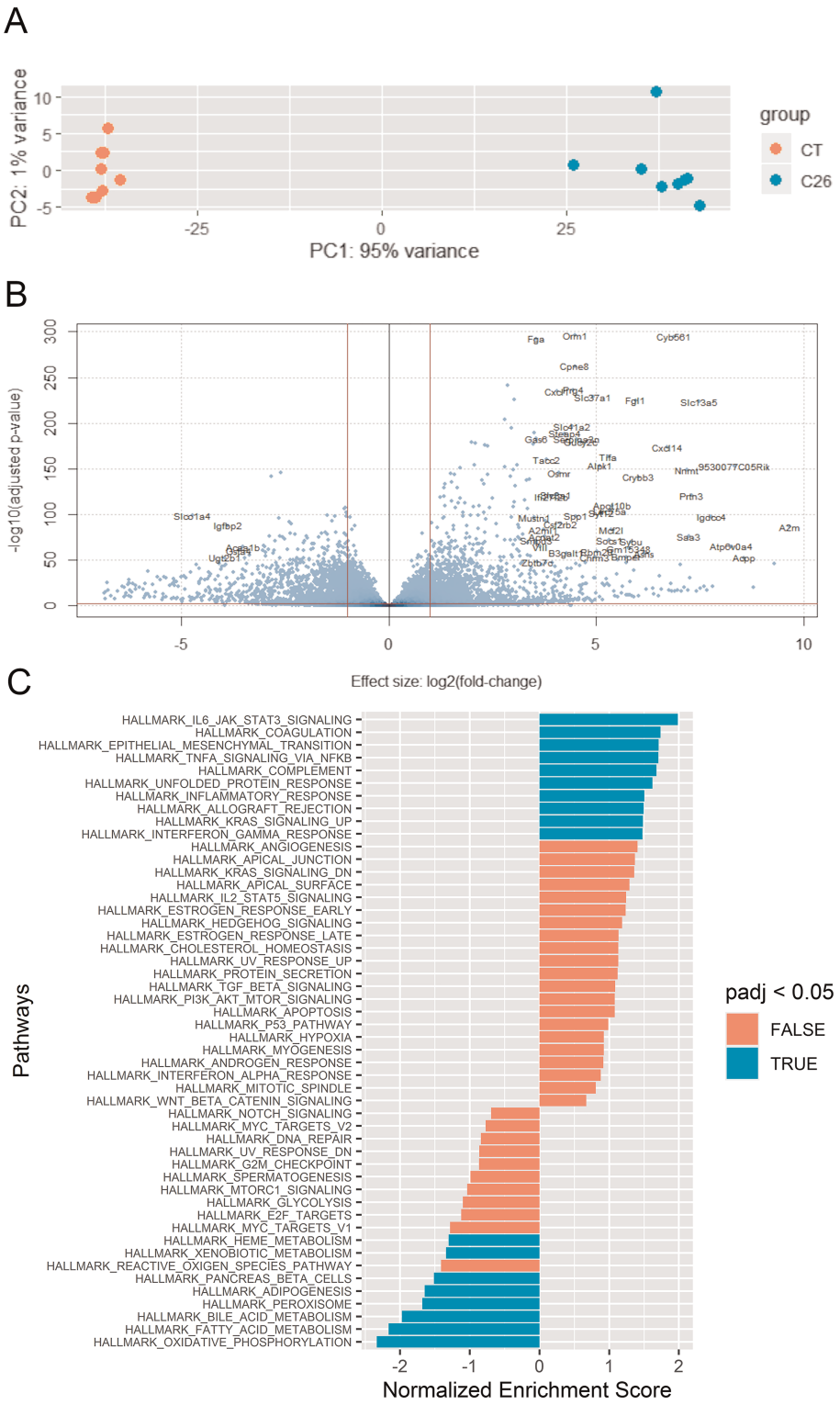

Figure 1 Hepatic whole transcriptome analysis in cachectic mice. (*A*) Principal component analysis of 22 389 expressed genes in sham-injected mice (CT) and in colon carcinoma 26 -transplanted mice (C26). (*B*) Volcano plot of genes differentially expressed in the liver of CT mice as compared with C26 mice [*P*adj $<$ 0.01, absolute $\log_2$(fold-change) $>$1]. (*C*) Table of the most significantly modified gene pathways between CT and C26 mice using gene set enrichment analysis. *N* = 8 mice per group.

C26 cachectic mice display increased circulating levels of bile acids and strong alterations in the bile acid enterohepatic cycle

Taking into consideration results from the hepatic whole transcriptome analysis and knowing the immunomodulatory potential of bile acids, we next investigated the bile acid metabolism of C26 cachectic mice in an independent experiment. First, we found that the level of FGF15, an intestinally produced protein upon the transcriptional control of intestinal FXR, a bile acid-responsive nuclear factor, was increased at the gene expression level in the ileum and at the protein level in the portal serum of cachectic mice (Supporting Information, *S1*). In the systemic serum of cachectic mice, we mainly found an increase in conjugated bile acids, which was significant for taurochenodeoxycholic acid (TCDCA), tauro-β-muricholic acid (TβMCA), and β-muricholic acid (βMCA), as well as a decrease in taurodeoxycholic acid (TDCA) (*Figure* 2A). Moreover, an increase in total hepatic bile acid levels was observed in cachectic mice (*Figure* 2B). Hepatic gene expression levels measured by qPCR showed a drastic reduction for genes involved in bile acid synthesis (*Cyp7a1*, *Cyp8b1*, *Cyp27a1*, and *Cyp7b1*) in cachectic mice, thereby confirming the results obtained by RNAseq in the first experiment (*Figure* 2C). Hepatic genes encoding taurine transporter (*Slc6a6*) and taurine synthesis (*Csad*) were also significantly reduced (*Figure* 2D). As for the two genes encoding for key enzymes involved in bile acid conjugation, expression levels of *Baat* were reduced in the liver of cachectic mice while *Bacs* was not affected (*Figure* 2E).

Taken together, these results demonstrate alterations in the bile acid enterohepatic cycle, as well as a clear rise of systemic and hepatic bile acid levels in cachectic mice which cannot be explained by the induction of bile acid synthesis and conjugation.

The hepatobiliary transport system and xenobiotic metabolism are altered in C26 cachectic mice

On the basis of our current knowledge regarding the consequences of bile acid accumulation in models of inflammation-induced cholestasis, we next decided to evaluate the hepatobiliary transport system integrity in cachectic mice. Results from the hepatic whole transcriptome analysis showed a down-regulation of most of the genes involved in bile secretion (*Bsep*, *Mrp2*, *Ae2*, *Mdr1α*, *Mdr2*, *Abcg2*, *Abcg5*, and *Abcg8*) and genes involved in bile acid uptake (*Ntcp*, *Oatp1b2*, and *Oatp2*) (*Figure* 3A, *Table* 1). Interestingly,

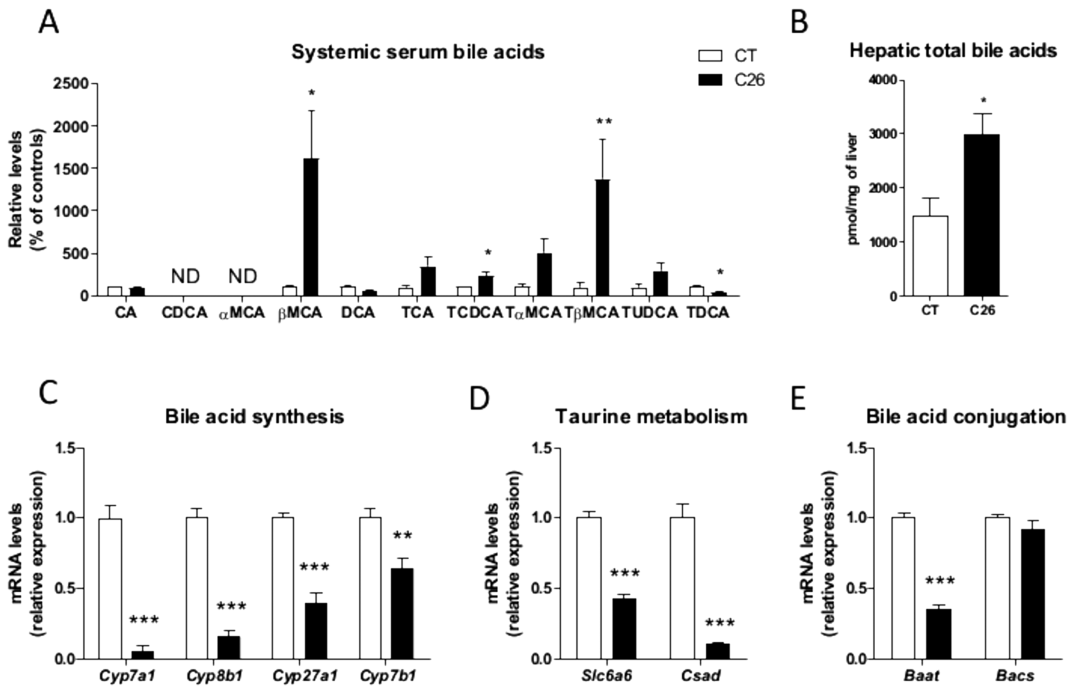

Figure 2 Bile acid pathways are altered in cachectic mice. (*A*) Bile acid profile in the systemic serum of colon carcinoma 26 -transplanted mice (C26) as compared with sham-injected mice (CT). (*B*) Total bile acid levels in the liver of C26 mice as compared with CT mice. (*C–E*) Hepatic mRNA expression levels. *Baat*, bile acid-CoA:amino acid *N*-acyltransferase; *Bacs*, Solute Carrier Family 27 Member 5; *Csad*, cysteine sulfinic acid decarboxylase; *Cyp27a1*, cytochrome P450 family 27 sub-family A member 1; *Cyp7a1*, cytochrome P450 family 7 sub-family A member 1; *Cyp7b1*, cytochrome P450 family 7 sub-family B member 1; *Cyp8b1*, cytochrome P450 family 8 sub-family B member 1; *Slc6a6*, solute carrier family 6 member 6. $N = 7–8$ mice per group; data are presented as mean ± SEM, $^{*}P < 0.05$, $^{**}P < 0.01$, $^{***}P < 0.001$.

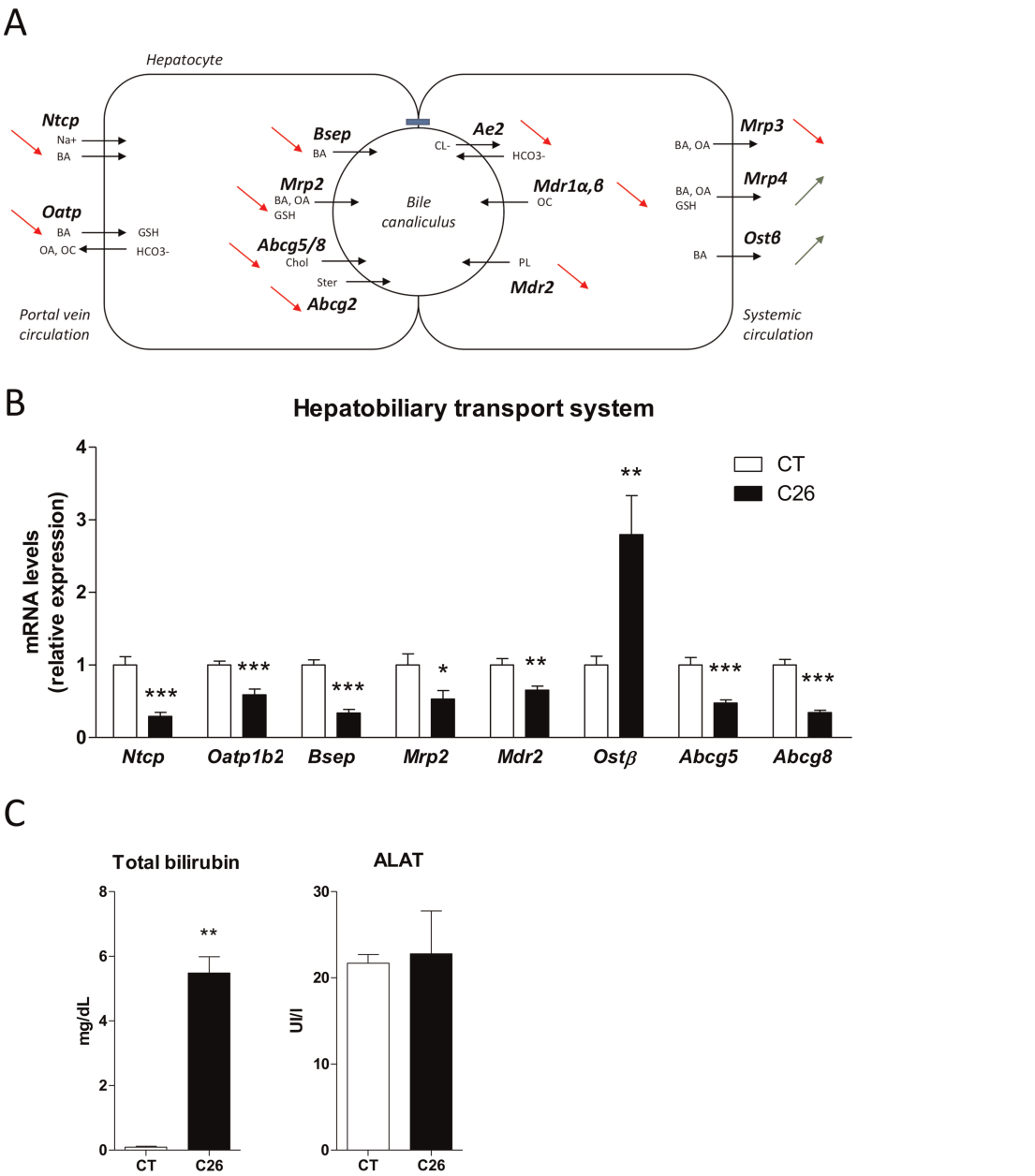

Figure 3 Impairment of the hepatobiliary transport system in cachectic mice. (*A*) Schematic illustration of alterations in the hepatobiliary transport system in cachectic mice revealed by hepatic whole transcriptome analysis of cachectic mice. (*B*) Hepatic mRNA expression levels of genes involved in the hepatobiliary transport system in the liver of colon carcinoma 26-transplanted mice (C26) as compared with sham-injected mice (CT). (*C*) Hepatic function parameters reflected by total bilirubin levels and alanine aminotransferase levels (ALAT) in the serum of C26 mice as compared with CT mice. Data from (*A*) and (*B*) come from independent experiments. *Abcg5*, ATP-binding cassette sub-family G member 5; *Abcg8*, ATP-binding cassette sub-family G member 8; *Bsep*, bile salt export pump; *Mdr2*, multidrug resistance protein 2; *Mrp2*, multidrug resistance-associated protein 2; *Ntcp*, Na(+)/taurocholate transport protein; *Oatp1b2*, organic anion transporter family member 1B2; *Ostβ*, organic solute transporter subunit beta; BA, bile acids; chol, cholesterol; CL-, chloride ion; GSH, glutathione; HC03-, ion bicarbonate; OA, organic anion; OC, organic cation; PL, phospholipids; ster, steroids. N = 7–8 mice per group; data are presented as mean ± SEM, $^{*}P < 0.05$, $^{**}P < 0.01$, $^{***}P < 0.001$.

adaptive mechanisms to counteract hepatic bile acid accumulation seem to be taking shape, including induction of alternative bile acid export to systemic circulation (*Mrp4* and *Ostβ*) (*Figure* 3A, *Table* 1). These changes were confirmed in an independent experiment using qPCR (*Figure* 3B). An analysis of hepatic function parameters in the serum of C26 mice showed no significant change in ALAT levels. However, a sharp increase was observed for total bilirubin levels (*Figure* 3C), which confirmed alterations of the hepatobiliary transport system in cachectic mice.

Table 1 Expression of genes involved in the hepatobiliary transport system of cachectic mice

Changes in cachectic mice vs. control mice	Log_2FC
Ntcp	−1.59
Oatp1b2	−1.44
Oatp2	−4.73
Bsep	−0.96
Mrp2	−1.48
Ae2	−0.50
Mdr1α	−1.11
Mdr2	−0.93
Abcg2	−0.92
Abcg5	−1.23
Abcg8	−1.49
Mrp3	−2.07
Mrp4	0.76
Ostβ	2.10

Values are log_2(fold-change) as compared with control mice ($n = 8$ per group).
All genes *P*adj < 0.001.

The hepatobiliary transport system is intrinsically related to inflammation through key regulatory transcription factors belonging to the family of nuclear receptors.[24] Focusing on genes related to these nuclear receptors, we noted a significant decrease of *Rxrβ*, *Rxrγ*, *Shp*, and *Car*, a slight increase was observed for *Hnf4a* and *Hnf1b*, while no significant difference was observed for *Rxrα*, *Fxr*, *Pxr*, and *Hnf1α* (*Table* 2). Taking a closer look, the vast majority of Phase I and II drug-metabolizing enzymes under the control of CAR and/or PXR[39] were substantially down-regulated (*Table* 3). This observation was further strengthened by the gene set enrichment analysis that highlighted xenobiotic metabolism as one of the most down-regulated pathways (*Figure* 1C) and by a previous study reporting a reduced hepatic drug metabolism in cachectic rats.[40]

Overall, these results highlighted a clear disruption of the hepatobiliary secretion, as well as a strong down-regulation of enzymes under the control of CAR and/or PXR in the liver of C26 cachectic mice.

Table 2 Expression of genes encoding nuclear receptors in cachectic mice

Changes in cachectic mice vs. control mice	Log_2FC
Rxrα	/
Rxrβ	−0.31
Rxrγ	−1.2
Fxr	/
Shp	−0.78
Car	−2.94
Pxr	/
Hnf4a	0.39
Hnf1a	/
Hnf1b	0.42

Values are log_2(fold-change) as compared with control mice ($n = 8$ per group).
All genes *P*adj < 0.001; /, genes not significantly affected.

Table 3 Expression of PXR and CAR target genes involved in xenobiotic metabolism (phase I and II enzymes) in cachectic mice

Changes in cachectic mice vs. control mice		Log_2FC
Regulated by CAR		
	Cyp1a1	−2.42
	Cyp1a2	−3.75
	Cyp2a4	−6.18
	Cyp2c29	−6.77
	Cyp2c37	−5.52
	Ugt1a6a	−1.31
	Ugt2b1	−3.95
Regulated by CAR/PXR		
	Cyp2b10	−3.85
	Cyp3a11	−4.99
	Ugt1a1	−2.21
	Ugt1a9	−4.64
	Gsta1	−6.43
	Gsta2	−6.86
	Sult2a1	/
	Sult1e1	5.19
Regulated by PXR		
	Ugt2b5	−2.37

Values are log_2(fold-change) as compared with control mice ($n = 8$ per group).
All genes *P*adj < 0.001; /, genes not significantly affected.

Hepatic inflammation and neutrophil recruitment are increased in C26 cachectic mice

One of the consequences of cholestasis is the induction of pro-inflammatory cytokines, as well as a recruitment of neutrophils in the liver.[27] To evaluate the inflammatory response in the liver of C26 mice, a western blot analysis of NFκB, a key regulator in immune response, has been carried out in nuclear extracts from the liver of C26 mice. We found a significant increase in the nuclear abundance of NFκB p65 in the liver of cachectic mice (*Figure* 4A). Results from the hepatic whole transcriptome analysis showed a strong up-regulation of inflammatory cytokines including *Il1β* and *Tnfα*, as well as chemokines and genes involved in neutrophil recruitment and adhesion including *Cxcl1*, *Cxcl2*, *Cxcl5*, *Ccl2*, *Icam1*, *Vcam1*, *Cxcr1/2*, and *Mmp8* in cachectic mice (*Table* 4). Of note, a modest increase was observed for *Adgre1*, and no difference was found for *Cd68*, two markers of macrophages (*Table* 4). Inflammatory infiltrates were found on haematoxylin and eosin-stained liver sections of C26 cachectic mice (Supporting Information, *Figure* S2). An immunohistochemistry against Ly6G was performed to study neutrophil recruitment and revealed a five-fold increase in the number of neutrophils present in liver sections of cachectic mice (*Figure* 4B).

Alterations in the bile acid metabolism and the hepatobiliary transport system correlate with the progression of cachexia in C26 cachectic mice

Next, we evaluated the time course of appearance of hepatic and bile acid alterations and associated it with the onset of

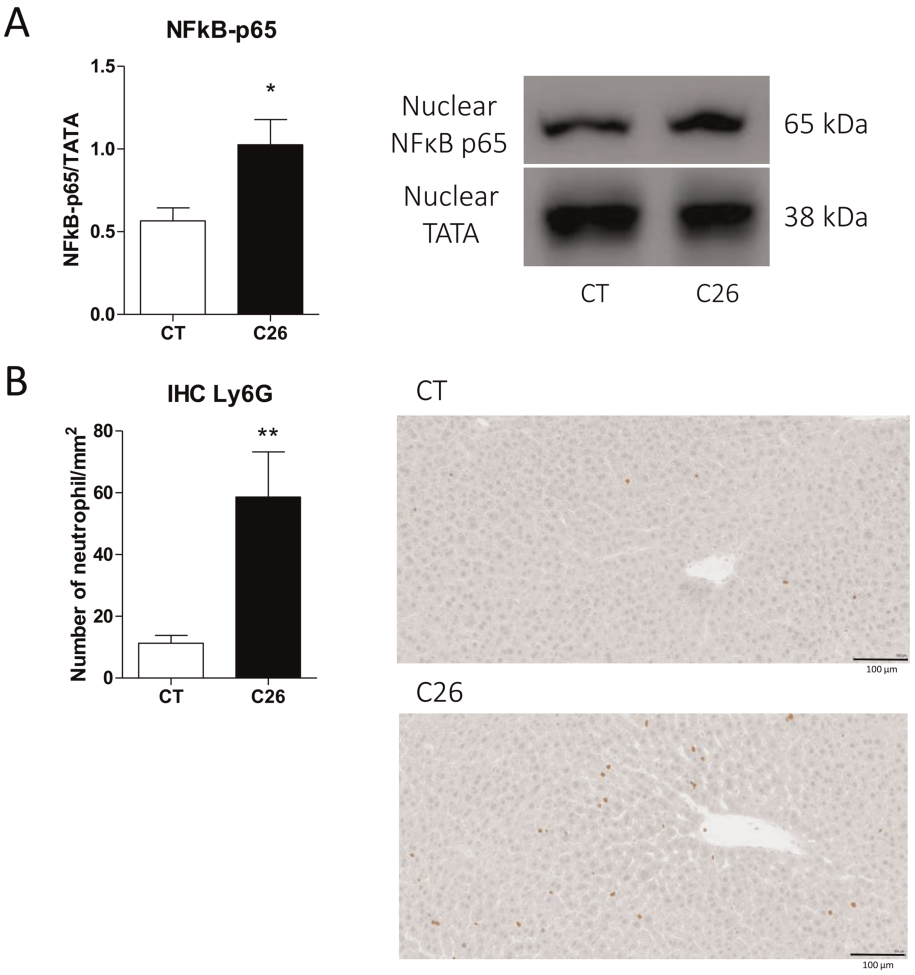

Figure 4 Hepatic inflammation in cachectic mice. (*A*) Western blot analysis of NFκB-p65 in nuclear fraction extracts from the liver of colon carcinoma 26-transplanted mice (C26) as compared with sham-injected mice (CT). (*B*) Immunohistochemistry of Ly6G, a specific marker of neutrophils, in the liver of C26 mice and CT mice. *N* = 6–8 mice per group; data are presented as mean ± SEM, $^{*}P < 0.05$, $^{**}P < 0.01$.

Table 4 Expression of genes involved in the inflammatory response and neutrophil recruitment in cachectic mice

Changes in cachectic mice vs. control mice	
	Log_2FC
Il6	/
IL1b	2.29
Tnfα	1.28
Ccl2	2.71
Cd68	/
Adgre1	0.45
Cxcl1	4.05
Cxcl2	5.00
Cxcl5	3.93
Icam1	2.31
Vcam1	1.15
Cxcr1	3.84
Cxcr2	3.76
Mmp8	7.13

Values are log_2(fold-change) as compared with control mice ($n = 8$ per group).
Tnfα and *Adgre1* have *P*adj < 0.05; /, genes not significantly affected; all other genes *P*adj < 0.001.

cachectic symptoms. In this experiment, we euthanized control and C26 mice ($n = 8$ mice per group) at three time points corresponding to different stages in the progression of cachexia: Day 8 with no weight loss and no reduced food intake, Day 9 with minor weight loss and first signs of anorexia (pre-cachexia), and Day 10 with marked reduced body weight and food intake (cachexia) (Supporting Information, *Figure* S3A). In line with these observations, the weights of subcutaneous adipose tissue and gastrocnemius were significantly decreased from Day 9 (Supporting Information, *Figure* S3A). At Day 8, the weight of the brown adipose tissue was already decreased (reflecting its activation), while the expression levels of genes involved in muscle atrophy (*Trim63* and *Fbxo32*) were already slightly induced in the gastrocnemius muscle (Supporting Information, *Figures* S3A and S3B). Regarding gene expression levels in the liver, most genes showed alterations at Day 8 and evolved continuously at Days 9 and 10 (*Cyp7a1*, *Cyp8b1*, *Cyp27a1*, *Oatp1b2*, *Ntcp*, *Cxcl2*,

Icam1, and *Mmp8*) (Supporting Information, *Figure* S3C). Gene expression levels of *Mrp2* and *Mdr2* were down-regulated from Day 9, while *Bsep* was up-regulated at Day 8 and down-regulated at Days 9 and 10. The down-regulation of *Cyp7b1* and up-regulation of *Ostβ* remained the same throughout the time course (Supporting Information, *Figure* S3C). Correlation analyses between cachectic parameters and hepatic gene expression levels in cachectic mice revealed that most genes involved in bile acid synthesis (*Cyp7a1*, *Cyp8b1*, and *Cyp27a1*) and hepatobiliary transport system (*Ntcp*, *Oatp1b2*, *Bsep*, *Mrp2*, and *Mdr2*) were positively correlated with the body weight and organ weights, especially with the brown adipose tissue weight (*Figure* 5A). Conversely, inflammatory genes (*Cxcl2*, *Icam1*,

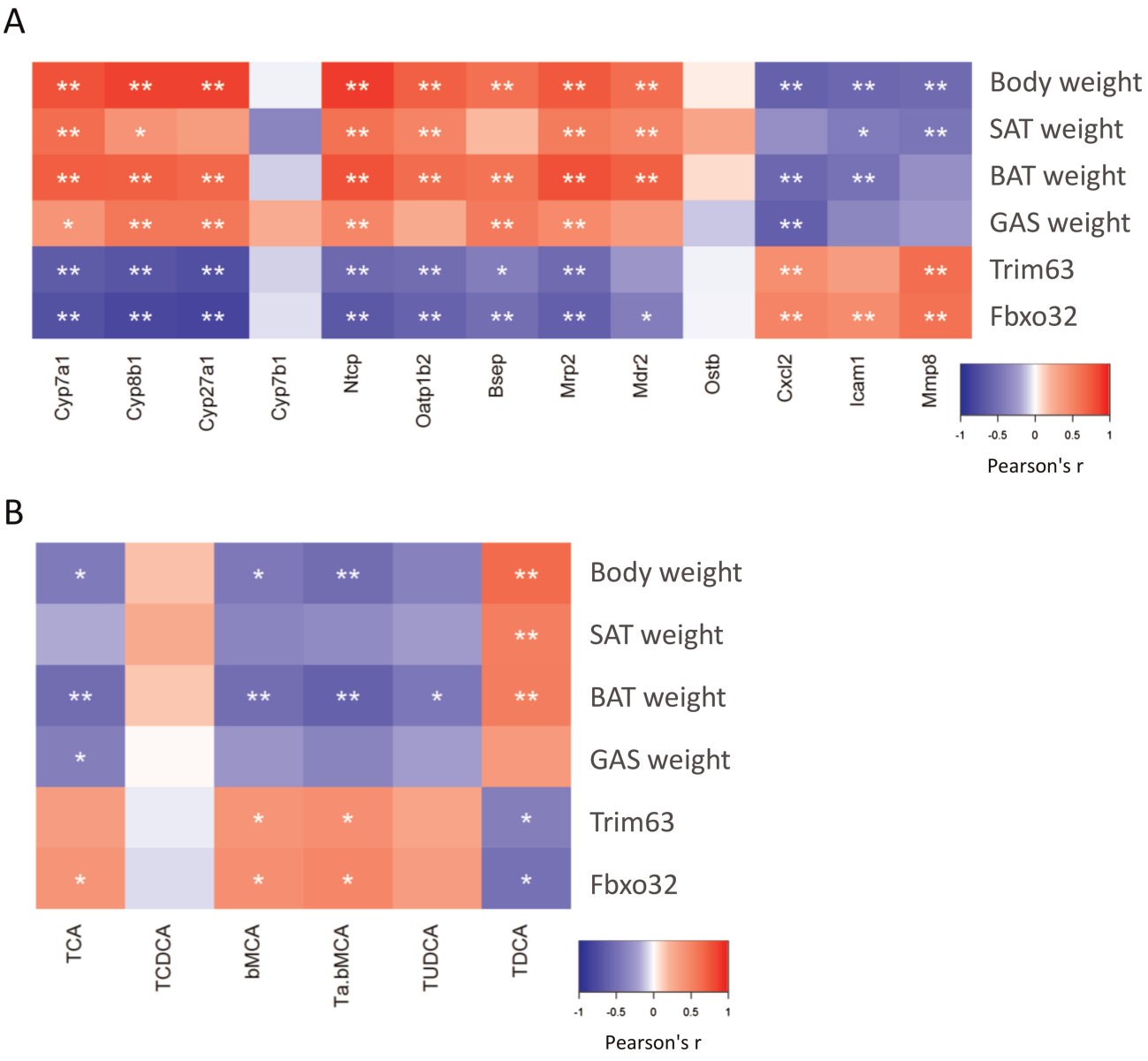

Figure 5 Strong association between hepatobiliary alterations and the progression of cachexia in colon carcinoma 26 (C26) mice. (*A*) Pearson correlations between cachectic parameters and hepatic gene expression levels in C26 mice euthanized at 8, 9 and 10 days after injection. (*B*) Pearson correlations between cachectic parameters and bile acid profiles in C26 mice euthanized at 8, 9, and 10 days after injection. BAT, brown adipose tissue; GAS, gastrocnemius; SAT, subcutaneous adipose tissue; *Bsep*, bile salt export pump; *Cxcl2*, C-X-C motif chemokine ligand 2; *Cyp27a1*, cytochrome P450 family 27 sub-family A member 1; *Cyp7a1*, cytochrome P450 family 7 sub-family A member 1; *Cyp7b1*, cytochrome P450 family 7 sub-family B member 1; *Cyp8b1*, cytochrome P450 family 8 sub-family B member 1; *Fbxo32*, F-box protein 32 (also known as Atrogin1); *Icam1*, intercellular adhesion molecule 1; *Mdr2*, multidrug resistance protein 2; *Mmp8*, matrix metallopeptidase 8; *Mrp2*, multidrug resistance-associated protein 2; *Ntcp*, Na (+)/taurocholate transport protein; *Oatp1b2*, organic anion transporter family member 1B2; *Ostβ*, organic solute transporter subunit beta; *Trim63*, tripartite motif containing 63 (also known as Murf1). *N* = 8 mice per group, **P* < 0.05, ***P*adj < 0.05.

DOI: 10.1002/jcsm.12652

and *Mmp8*) were inversely correlated with these parameters (*Figure* 5A). Regarding the bile acid profile, we found a significant increase in total bile acid levels in the liver of mice euthanized at Day 10 (Supporting Information, *Figure* S4A). In line with these observations, taurocholic acid (TCA) and Tα/βMCA increased at Day 10, while βMCA increased from Day 9 and TDCA decreased from Day 8 (Supporting Information, *Figure* S4A). Most bile acids were negatively correlated with the body and organ weights, especially with the brown adipose tissue weight (*Figure* 5B). Inversely, TDCA was strongly positively correlated with the body and organ weights (*Figure* 5B). Taken together, these results highlight the early and progressive nature of hepatic alterations in cancer cachexia and clearly demonstrate the existence of a strong association between hepatobiliary alterations and the progression of cachexia in C26 mice.

Cholestyramine treatment counteracts alterations in hepatic bile acid profile and reduces hepatic inflammation in C26 cachectic mice

We next investigated the contribution of bile acids to the hepatic alterations observed in cancer cachexia using a bile acid sequestrant, cholestyramine, to decrease bile acid reuptake and reduce the bile acid load in the enterohepatic circulation. Therefore, a group of cachectic mice received cholestyramine, at 2% w/w in their diet, from Days 1 to 10 after cell injection (C26-CHO group). *Fgf15*, a key marker of treatment efficacy, was strongly reduced in the ileum of cachectic mice treated with cholestyramine (Supporting Information, *Figure* S5A). Regarding tumour weight and food intake, results showed no significant difference between C26 and C26 mice treated with cholestyramine (Supporting Information, *Figure* S5B). Despite no significant effect of cholestyramine on absolute body weight evolution, the body weight loss rate was slowed down (Supporting Information, *Figure* S5C). As a recent report showed that supraphysiological levels of bile acids can induce muscle atrophy *in vitro* through *GPBAR1*,[41] we analysed the expression of muscle atrophy markers in the gastrocnemius muscle and we found out a downward trend for all markers, that reaches significance for *Ctsl* (Supporting Information, *Figure* S5D). Knowing that bile acids can activate *GPBAR1* in the brown adipose tissue and lead to increased energy expenditure,[42] we also investigated markers of thermogenesis in the brown adipose tissue of C26 mice treated with cholestyramine. We found reduced expression levels for *Ucp1* and *Lpl* in the brown adipose tissue of C26-CHO mice as compared with C26 mice (Supporting Information, *Figure* S5E).

The hepatic bile acid profile displayed enhanced levels of tauroconjugated bile acids including TCA, Tα/βMCA, tauroursodeoxycholic acid (TUDCA), tauro-ω-muricholic acid (TωMCA), and βMCA, while decreased TDCA levels in cachectic mice were observed (*Figure* 6A). Cholestyramine treatment significantly counteracted the hepatic increase of βMCA, Tα/βMCA, TUDCA and TωMCA as compared with those in untreated C26 mice (*Figure* 6A).

To define the contribution of altered bile acid levels to hepatic disturbances associated with cancer cachexia, a hepatic whole transcriptome analysis was performed, comparing C26 and C26-CHO mice (eight mice per group). Our analysis highlighted 322 genes significantly affected by cholestyramine administration ($P\text{adj} < 0.05$, full list in the Supporting Information, *Table* S4). Among these 322 genes, 48 genes were induced, and 10 genes were repressed with an absolute $\log_2(\text{fold-change}) > 1$. Volcano plot of differentially expressed hepatic genes between untreated cachectic mice and cholestyramine-treated cachectic mice clearly showed that *Cyp7a1* and *Cyp8b1* were the two major genes induced upon cholestyramine treatment (*Figure* 6B). Gene set enrichment analysis revealed that genes involved in fatty acid metabolism, oxidative phosphorylation, xenobiotic metabolism, bile acid metabolism, adipogenesis, peroxisome, reactive oxygen species pathway, and heme metabolism were up-regulated by cholestyramine (*Figure* 6C), while the same set of genes were down-regulated in cachectic mice vs. healthy mice (*Figure* 1C). Conversely, genes implicated in unfolded protein response, IL-6/JAK/STAT-3 signalling, TNFα signalling via NFκB, inflammatory response, KRAS up-signalling were down-regulated in cholestyramine-treated mice (*Figure* 6C), while these genes were up-regulated in cachectic mice as compared with those in healthy mice (*Figure* 1C). Of note, the expression levels of genes implicated in the hepatobiliary transport system were not significantly affected by the cholestyramine treatment (except a slight increase of *Oatp2* and *Mrp2*) (*Table* 5). Nevertheless, cholestyramine treatment significantly counteracted the enhanced expression of most of the genes involved in inflammation and neutrophil recruitment including *Tnfα*, *Cxcl1*, *Cxcl2*, *Icam1*, and *Mmp8*, with key results from the hepatic whole transcriptome analysis being confirmed by qPCR (*Figure* 6D).

Altogether, these data clearly demonstrate that cholestyramine reduces hepatic inflammation in cachectic mice and therefore that bile acids contribute to hepatic inflammation in this context. Our analyses also revealed minor effects of cholestyramine treatment on markers of cancer cachexia, including muscle atrophy and thermogenesis. Although these changes are minor, these results reinforce the hypothesis that targeting bile acids could effectively affect cachexia.

Anorexia does not drive bile acid alterations in C26 cachectic mice

Severe acute malnutrition has been associated with altered bile acid homeostasis.[43] We therefore sought to evaluate whether the reduced food intake observed in the late stage

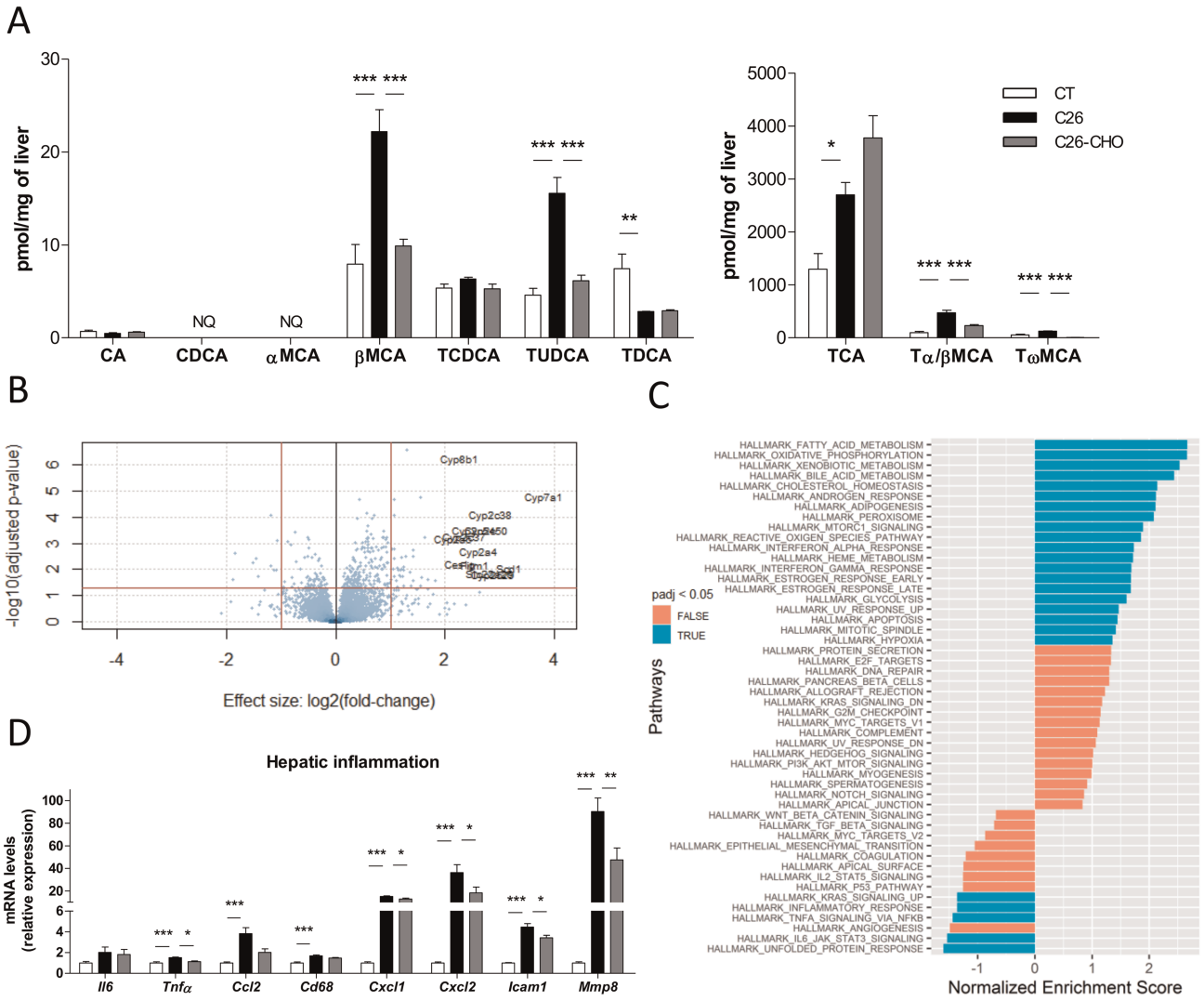

Figure 6 Cholestyramine treatment counteracts alterations in hepatic bile acid profile and reduces hepatic inflammation in cachectic mice. (*A*) Hepatic bile acids profile in sham-injected mice (CT), in untreated colon carcinoma 26-transplanted mice (C26) and in C26-transplanted mice receiving cholestyramine in their diet (C26-CHO). (*B*) Volcano plot of genes differentially expressed in the liver of C26-CHO mice as compared with C26 mice [*Padj* < 0.05, absolute $\log_2$(fold-change) >1]. (*C*) Table of the most significantly modified gene pathways between C26 and C26-CHO mice using gene set enrichment analysis. *(D)* Hepatic mRNA expression levels of genes involved in inflammation in CT, C26 and C26-CHO. *Ccl2*, C-C motif chemokine ligand 2; *Cd68*, CD68 molecule; *Cxcl1*, C-X-C motif chemokine ligand 1; *Cxcl2*, C-X-C motif chemokine ligand 2; *Icam1*, intercellular adhesion molecule 1; *Il6*, interleukin-6; *Mmp8*, matrix metallopeptidase 8; *Tnfα*, tumour necrosis factor. *N* = 7–8 mice per group; data are presented as mean ± SEM, $^*P < 0.05$, $^{**}P < 0.01$, $^{***}P < 0.001$ vs. C26.

of the disease could also contribute to the altered bile acid pathways and the inflammation found in cachectic mice. To isolate the impact of anorexia, two groups of healthy mice were calorie restricted to the amount of food consumed either by the CT group or the C26 group (an approach called pair-feeding). The reduced food intake did not explain the modulation, in cachectic mice, of ileal *Fgf15* as well as hepatic *Cyp7a1*, *Cyp8b1*, *Ntcp*, *Cxcl2* and *Icam1* (Supporting Information, *Figure* S6). The only prominent change was a decrease of *Bsep* in mice pair-fed to the C26 group vs. mice pair-fed to the CT group, with a fold-change similar to the one observed in cachectic mice (Supporting Information, *Figure* S6). Altogether, these results establish that anorexia does not play a major role in bile acid alterations observed in cachectic mice.

IL-6 is the main driver of hepatic alterations in C26 cachectic mice

To evaluate the tumour-host crosstalk, we looked for a mediator secreted directly by the tumour or by the host in response to the tumour presence and which could directly target the liver. As IL-6 is considered as one of the key

Table 5 Expression of genes involved in the hepatobiliary transport system of cachectic mice receiving cholestyramine in their diet

Changes in cholestyramine-treated cachectic mice vs. cachectic mice		
	Log_2FC	*P*adj
Ntcp	/	/
Oatp1b2	/	/
Oatp2	1.03	<0.05
Bsep	/	/
Mrp2	0.39	<0.05
Ae2	/	/
Mdr1α	/	/
Mdr2	/	/
Abcg2	/	/
Abcg5	/	/
Abcg8	/	/
Mrp3	/	/
Mrp4	/	/
Ostβ	/	/

Values are log_2(fold-change) as compared with cachectic mice ($n = 8$ per group). /, genes not significantly affected.

mediators of cachexia and displays hepatic acute phase response stimulating properties in cancer cachexia,[44,45] we next evaluated the role of IL-6 on hepatic alterations using a neutralizing antibody against IL-6. Therefore, a group of C26 cachectic mice received a neutralizing IL-6 antibody (anti-IL-6), and another group received an IgG isotope control (IgG) to dissociate the effect of the antibody administration. The anti-IL-6 antibody administration counteracted the 16-fold increase in IL-6 levels, leading to an almost complete maintenance of body weight and food intake and preventing the induction of markers of muscle atrophy.[46] Furthermore, administration of the IL-6 antibody counteracted expression levels of several genes involved in the hepatobiliary transport system including *Ntcp*, *Oatp1b2*, *Ostβ*, *Abcg5*, and *Abcg8*, while *Bsep* was not significantly affected (*Figure* 7A). In addition, the expression levels of the two main genes driving bile acid synthesis, *Cyp7a1* and *Cyp8b1*, were restored after anti-IL-6 administration (*Figure* 7B). Similar results were observed regarding key inflammatory markers, including *Il1β*, *Icam1*, *Cxcl1*, and *Cxcl2* (*Figure* 7C).

These results demonstrate that IL-6 is a key mediator regulating gene expression involved in the cholestasis found in C26 cachectic mice.

Similar hepatic alterations are found in LLC cachectic mice

As IL-6 is a mediator that particularly drives cachexia observed in the C26 model, we investigated whether we could observe similar cholestasis indicators in another well-established model of cancer-related cachexia, the LLC model. In this model, hepatic expression levels of key genes involved in the hepatobiliary transport system (*Ntcp*, *Mrp2*, and *Ostβ*) were significantly reduced, with no impact on *Bsep* (*Figure* 8A). The down-regulated expression of *Ostβ* suggests that alternative routes of basolateral bile acid efflux do not seem to be established yet. Down-regulation of genes involved in bile acid synthesis, except for *Cyp7a1* (*Figure* 8B), and up-regulation of similar pro-inflammatory cytokines (*Il6*, *Cxcl1*, *Cxcl2* and *Mmp8 Figure* 8C) were also observed in the liver of LLC mice. However, *Il1β* and *Tnfα* were not significantly affected (*Figure* 8C). The difference observed for *Cyp7a1* probably stems from the fact that the C26 model, unlike the LLC model, is characterized by high circulating levels of IL-6 and hepatic expression of IL-1β, which may repress *Cyp7a1* directly through the JNK/c-Jun signalling pathway.[47] Altogether, these results extend our findings to another preclinical model of cancer cachexia.

Alteration of serum bile acids correlates with inflammatory markers in cachectic and non-cachectic colorectal cancer patients

Finally, we investigated the translational value of our findings by analysing the serum bile acid profile in a cohort of 43 cachectic colorectal cancer patients and 51 non-cachectic colorectal cancer patients (patients and tumour characteristics in the Supporting Information, *Table* S5). An upward trend was observed for most bile acids, and significant increased levels were found for TCDCA and glycoursodeoxycholic acid in cachectic patients as compared with those in non-cachectic patients (*Figure* 9A). Concordantly, total bile acid quantification in the serum of cancer patients highlighted significantly higher levels for cachectic patients (*Figure* 9B). Serum IL-6 and total bilirubin levels were also increased while the alkaline phosphatase activity was not affected (Supporting Information, *Table* S5). Sex-corrected and age-corrected correlations between bile acids and several clinical parameters showed as a whole that bile acids positively correlate with clinical markers increasing in cachexia (e.g. C-reactive protein, IL-6, and weight loss) while they are negatively associated with clinical markers decreasing in cachexia (e.g. lean mass, albumin, and survival) (*Figure* 9C). The strongest correlations were found between conjugated bile acids and C-reactive protein, a key inflammatory marker produced in the liver and a negative predictive biomarker in cancer cachexia[48] (TCDCA $\rho = 0.36$, TDCA $\rho = 0.26$, GCDCA $\rho = 0.27$).

Discussion

Cancer cachexia is presently considered as a multi-organ syndrome and an improved knowledge regarding the contribution of organs other than the muscle to the pathogenesis of cancer cachexia is starting to emerge.[1,2] Hence, given that the liver was proposed to play a major role in cachexia,[1,8,17,18]

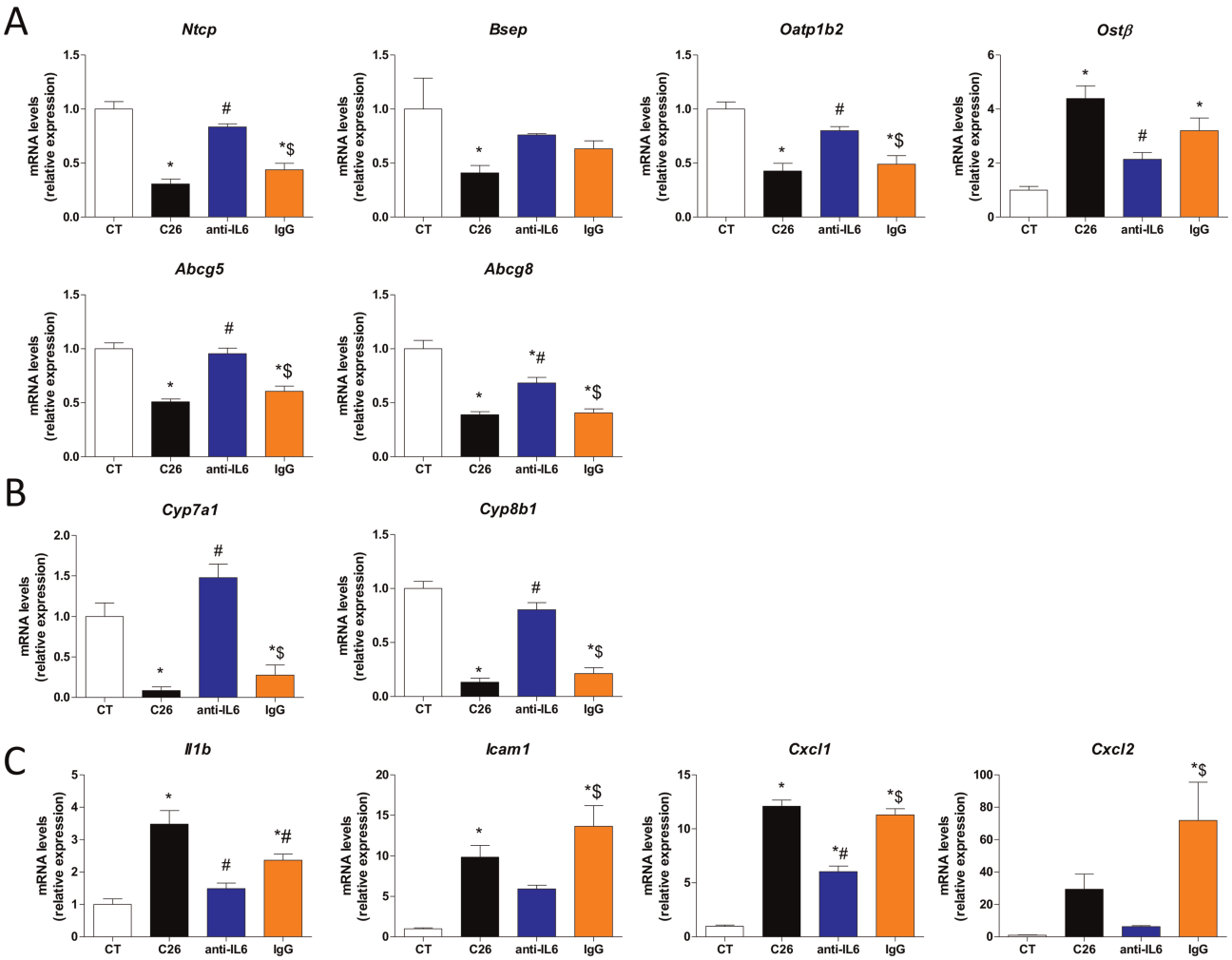

Figure 7 IL-6 is the main driver of hepatic alterations in cachectic mice. (*A*) Hepatic mRNA expression levels of genes involved in the hepatobiliary transport system in the liver of colon carcinoma 26-transplanted mice treated with phosphate-buffered saline (C26), a neutralizing antibody targeting IL-6 (anti-IL-6) or an isotope control (IgG) and control mice injected with phosphate-buffered saline (CT). (*B*) Hepatic mRNA expression levels of genes involved in bile acid synthesis in the liver of CT, C26, anti-IL-6 and IgG mice. (*C*) Hepatic mRNA expression levels of genes involved in inflammatory response in the liver of CT, C26, anti-IL-6 and IgG mice. *Abcg5*, ATP-binding cassette sub-family G member 5; *Abcg8*, ATP-binding cassette sub-family G member 8; *Bsep*, bile salt export pump; *Cxcl1*, C-X-C motif chemokine ligand 1; *Cxcl2*, C-X-C motif chemokine ligand 2; *Cyp7a1*, cytochrome P450 family 7 sub-family A member 1; *Cyp8b1*, cytochrome P450 family 8 sub-family B member 1; *Il1b*, interleukin-1β; *Icam1*, intercellular adhesion molecule 1; *Ntcp*, Na(+)/taurocholate transport protein; *Oatp1b2*, organic anion transporter family member 1B2; *Ostβ*, organic solute transporter subunit beta. $N = 7–8$ mice per group; data are presented as mean ± SEM. One-way ANOVA with Tukey's post-tests. *$P < 0.05$ vs. CT, #$P < 0.05$ vs. C26, $$P < 0.05$ vs. anti-interleukin 6 (IL-6).

we decided to investigate the mechanisms underlying hepatic alterations in cancer cachexia.

Altogether, our multiple independent experiments clearly establish that bile acid pathways are deeply disrupted in cachectic mice and cancer patients. In particular, increased levels of conjugated bile acids were found in the serum of cachectic cancer patients as well as in the serum and liver of cachectic mice. The most relevant explanation for such accumulation of bile acids comes from studies in rodent models of endotoxemia. In these studies, pro-inflammatory cytokines, including TNFα, IL-1β, and IL-6, induce a strong reduction of transporters involved in bile formation and bile acid secretion, leading to an accumulation of bile acids in the liver.[49–51] In a similar way, our gene expression level analyses point out that in cachectic mice, the hepatobiliary secretion is disturbed. In accordance with this result, we show in cachectic mice that adaptive mechanisms were set up to counteract this bile acid accumulation by repressing bile acid synthesis and by enhancing alternative routes of basolateral bile acid efflux (*Mrp4* and *Ostβ*).[25] Such basolateral efflux may contribute to the accumulation of tauroconjugated bile acids in the systemic circulation. A classical consequence of inflammation-induced cholestasis is the production by the hepatocytes of pro-inflammatory mediators and neutrophil

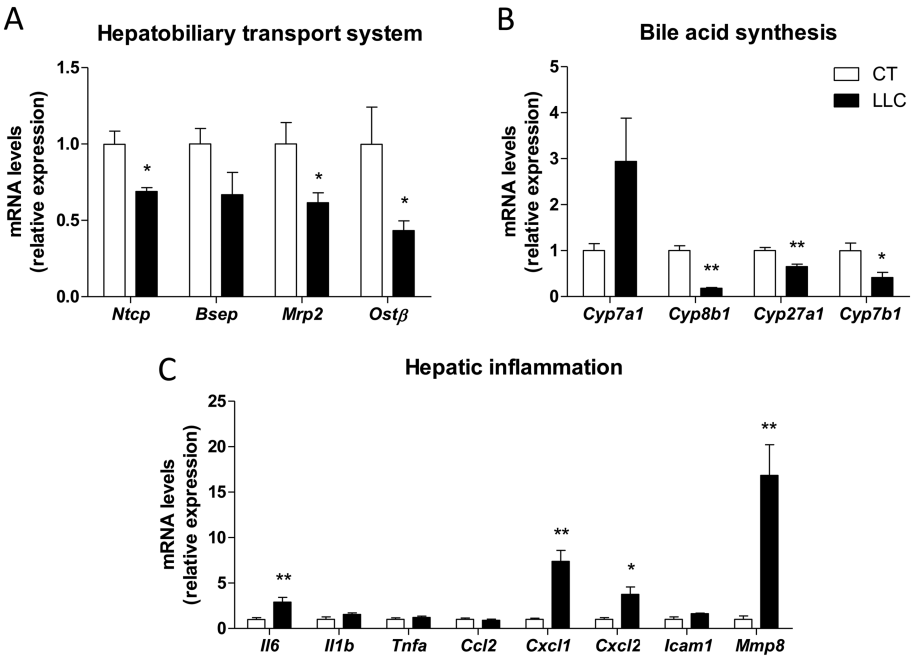

Figure 8 Similar hepatic alterations were found in cachectic Lewis lung carcinoma-injected mice. (*A*) Hepatic mRNA expression levels of genes involved in the hepatobiliary transport system in Lewis lung carcinoma -injected mice (LLC) as compared with sham-injected mice (CT). (*B*) Hepatic mRNA expression levels of genes involved in bile acid synthesis in the liver of LLC mice as compared with CT mice. (*C*) Hepatic mRNA expression levels of genes involved in inflammation in the liver of LLC mice as compared with CT mice. *Bsep*, bile salt export pump; *Ccl2*, C-C motif chemokine ligand 2; *Cxcl1*, C-X-C motif chemokine ligand 1; *Cxcl2*, C-X-C motif chemokine ligand 2; *Cyp27a1*, cytochrome P450 family 27 sub-family A member 1; *Cyp7b1*, cytochrome P450 family 7 sub-family B member 1; *Cyp7a1*, cytochrome P450 family 7 sub-family A member 1; *Cyp8b1*, cytochrome P450 family 8 sub-family B member 1; *Icam1*, intercellular adhesion molecule 1; *Il6*, interleukin-6; *Il1b*, interleukin-1β; *Mmp8*, matrix metallopeptidase 8; *Mrp2*, multidrug resistance-associated protein 2; *Ntcp*, Na(+)/taurocholate transport protein; *Ostβ*, organic solute transporter subunit beta; *Tnfα*, tumour necrosis factor. *N* = 5–6 mice per group; data are presented as mean ± SEM, $*P < 0.05$, $**P < 0.01$.

recruitment.[27–29] Such features were observed in cachectic mice, with (i) an up-regulation of IL-6/JAK/STAT-3 signalling, TNFα signalling via NFκB and inflammatory response revealed by whole transcription analysis, (ii) increased expression levels of pro-inflammatory cytokines, (iii) enhanced nuclear levels of NFκB, and (iv) increased number of neutrophils recruited to the liver of C26 cachectic mice. Taken together, these results clearly reveal the development of cholestasis in the context of cancer cachexia.

The administration of an anti-IL-6 antibody counteracts the changes in the expression of genes involved in hepatobiliary transport and bile acid synthesis, demonstrating the causal role played by the systemic inflammation induced by the tumour on the development of cholestasis in cancer cachexia. Mechanisms underlying how inflammation represses the hepatobiliary transport system request a complex regulation and involve numerous nuclear receptors at multiple levels.[24,25] A consensus seems to emerge from several studies and involves a reduction of mRNA and protein expression of RXR, the obligate heterodimer partner of Class II nuclear receptors (known as LXR, FXR, RAR, PPAR, CAR, and PXR),[52] as well as HNF4α.[53] As an example, RXRα:RARα complex was shown to be a key regulator of NTCP and MRP2 in LPS-treated rodents.[49,54] Interestingly, gene expressions of *Rxrβ* and *Rxrγ* were significantly decreased in the liver of cachectic mice [$\log_2$(fold-change) −0.31 and −1.2, respectively], whereas *Rxrα* was not significantly affected (*Table* 2). Further studies are needed to clearly demonstrate the contribution of RXR in reducing hepatobiliary transport in the context of cancer cachexia.

Bilirubin accumulation in the serum of C26 cachectic mice is another key feature of cholestasis and was associated in our experiments with the hepatic down-regulation of *Ugt1a1* (under the regulation of CAR), involved in bilirubin conjugation, and *Mrp2*, involved in conjugated-bilirubin bile secretion. Interestingly, cholestyramine treatment significantly counteracted expression levels of *Car*, *Ugt1a1*, and *Mrp2*, suggesting a potential protective effect through reactivation of genes involved in xenobiotic metabolism and liver detoxification. Indeed, a down-regulation of CAR and PXR is found in LPS-treated rodents,[55] and CAR activation has already shown hepatoprotective effects against cholestasis induced by bile duct ligation, a mouse model also characterized by a reduced xenobiotic detoxification pathway.[56,57]

Cholestyramine treatment also significantly reduced the levels of most tauroconjugated bile acids in the liver, with

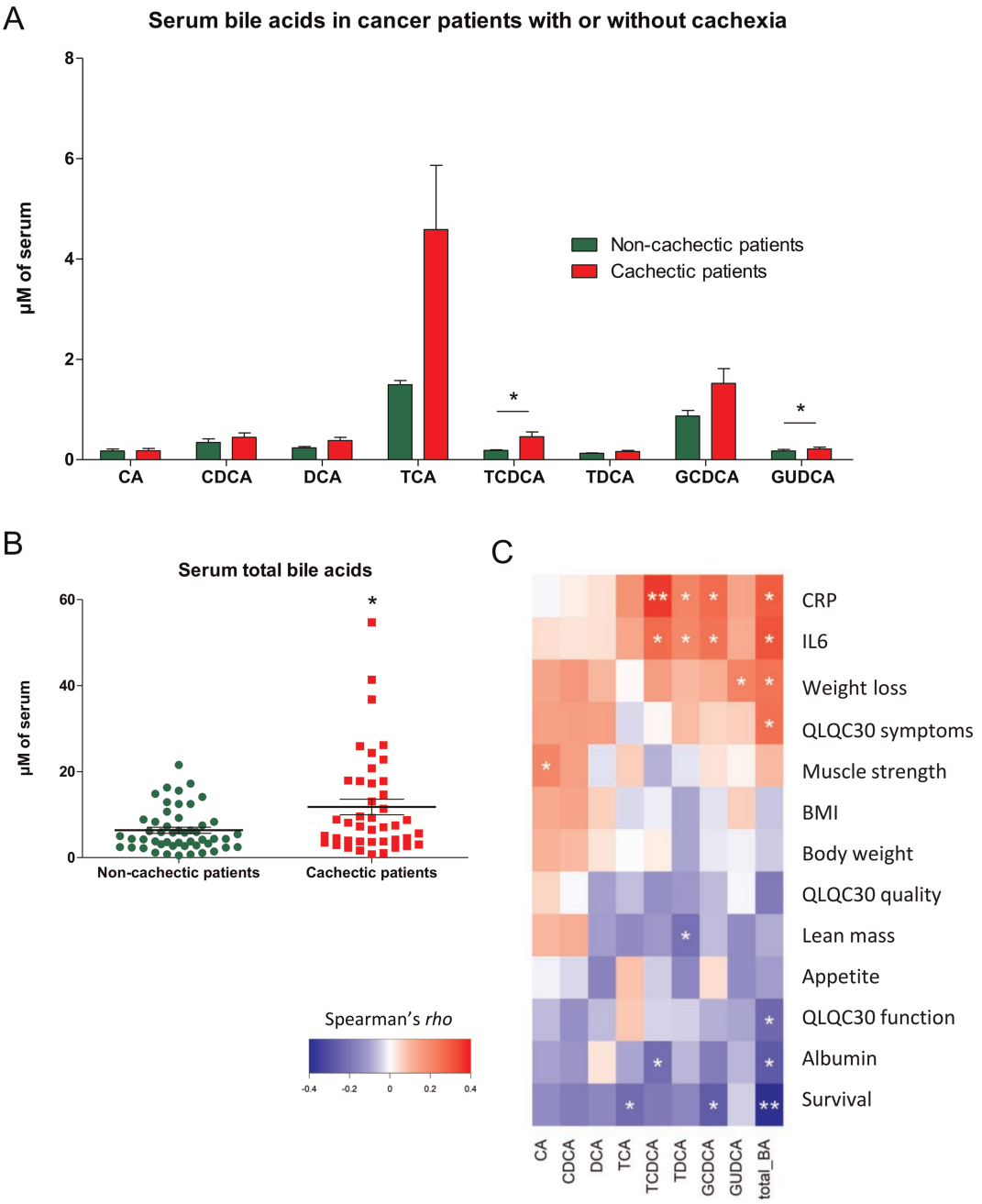

Figure 9 Alteration of serum bile acids correlates with inflammatory markers in cachectic and non-cachectic colorectal cancer patients. (*A*) Bile acid profile in the serum of cachectic and non-cachectic colorectal cancer patients. (*B*) Serum total bile acid levels in cachectic and non-cachectic colorectal cancer patients. (*C*) Partial Spearman rank-based correlations between serum bile acids and clinical parameters (corrected for age and sex). $N = 51$ non-cachectic patients, 43 cachectic patients, mean ± SEM, $^{*}P < 0.05$, $^{**}P\text{adj} < 0.05$. BMI, body mass index; CRP, C-reactive protein.

the exception of TCA, whereas hepatic transcriptome analysis shows that *Cyp7a1* and *Cyp8b1*, two major genes involved in the classical pathway of bile acid synthesis, were induced upon cholestyramine treatment. Altogether, these results indicate an activation of the classical bile acid synthesis pathway upon cholestyramine allowing the production of cholic acid and TCA from cholesterol to overcome the loss of bile acids induced by the administration of cholestyramine. Induction of the classical pathway of bile acid synthesis during bile acid sequestration has already been reported in humans[58] and in mice.[59] Importantly, cholestyramine treatment significantly down-regulated the expression of genes involved in inflammatory pathways including IL-6/JAK/STAT-3 signalling, TNFα signalling via NFκB and inflammatory response.

Mechanisms by which bile acids induce the production of inflammatory cytokines in hepatocytes remain not fully elucidated. However, it seems to be partially dependent on the transcription factor early growth response 1 (Egr1) and on the activation of the Toll-like receptor 9 through the endoplasmic reticulum stress and mitochondrial damages.[28,29] Of note, cholestyramine counteracted the enhanced production of pro-inflammatory cytokines without any effect on the expression of key genes involved in the hepatobiliary transport system. A previous study showed that another bile acid sequestrant, colesevelam, can attenuate liver inflammation in cholestatic Mdr2$^{-/-}$ mice. Similarly to our study, the hepatoprotective effects of colesevelam were associated with the modulation of bile acid composition without any effect on the bile flow.[60] The hepatic expression of *Cox2*, the key enzyme responsible for the production of prostaglandins, has been shown to be induced in cachectic mice and to contribute to local and systemic inflammation.[61–63] However, in our hands, *Cox2* expression was not induced in C26 cachectic mice (Supporting Information, *Table* S2) and not affected by cholestyramine treatment, which precludes its implication in bile acid-related inflammation in this context.

Our correlation analyses established the strong association over time between the alterations in the hepatobiliary system and the bile acid pathway on the one hand, and cachectic features on the other hand (muscle atrophy and thermogenesis). Considering that the cholestyramine exerted a minor effect on such classical cachectic features, we propose that targeting bile acids may generate benefits beyond the hepatic compartment. In our cohort of 94 colorectal cancer patients, serum total bile acid levels were significantly higher in cachectic cancer patients, and bile acid levels were strongly correlated to systemic inflammation in these patients, which further strengthen our preclinical results. Our knowledge about hepatic inflammation in human cancer cachexia is particularly scarce. Previous studies reported liver macrophage infiltration and down-regulation of IL-4 gene expression in liver sections of cachectic pancreatic cancer patients.[64,65] A mild cholestasis was documented in a cohort of cachectic and non-cachectic patients with various cancer types and was characterized by an increase in serum levels of alkaline phosphatase and gamma-glutamyl transpeptidase.[66] In our cohort, the alkaline phosphatase activity was not affected by the cachectic status of the patient while total bilirubin, another marker of cholestasis, was mildly increased. If an alteration of the hepatobiliary transport is confirmed in independent cohorts, restoring the bile acid secretion using choleretic compounds may represent an innovative strategy to alleviate cancer cachexia. First, such impaired bile acid secretion in cachectic cancer patients could have serious consequences on lipid and fat-soluble vitamin digestion and might thereby worsen the cachectic phenotype. Second, previous work from our team shows that the gut microbiota appears as a novel actor in cancer cachexia.[67–69] Based on our knowledge of the bile acids-microbiota crosstalk,[70,71] we speculate that the disruption in the hepatobiliary secretion may also contribute to the gut bacterial dysbiosis found in cancer cachexia. Vice versa, the gut bacterial dysbiosis may contribute to the altered bile acid profile. In favour of this last hypothesis, we observed a strong and early decrease in TDCA, a main secondary bile acid arising from the bacterial transformation of TCA.

In conclusion, our study highlights a cholestasis in cancer cachexia and unequivocally demonstrates, in this context, that systemic inflammation strongly contributes to this impairment of the hepatobiliary transport system. Targeting the enterohepatic circulation, we show that bile acids contribute to hepatic inflammation and disorders. Altogether, our work highlights a vicious circle between bile acids and inflammation and paves the way to new therapeutic strategies targeting bile acids to control hepatic inflammation and metabolic disturbances in cancer cachexia.

Funding

M.M.T. is a research fellow from the FRIA (FRIA, F.R.S.-FNRS). M.S. is a postdoctoral fellow from the F.R.S.-FNRS-*Télévie*. M.R., G.D. and J.G. are doctoral fellows from the F.R.S-FNRS; A.E. is a research associate from the F.R.S.-FNRS; P.D.C. is a senior research associate from the F.R.S.-FNRS. This study was supported by the F.R.S.-FNRS (CDR J.0019.18, MIS F.4512.20), the Télévie (Intercachectomics consortium), and the Louvain Foundation, through funding awarded to L.B.B. L.B.B. is also the recipient of subsidies from the FSR [Fonds Spéciaux de la Recherche, UCLouvain, including the Action de Recherche Concertée LIPOCAN (19-24.096)]. This work benefitted from the support of the *Institut Mérieux* through the allocation of the Pharmabiotics Young Investigator Award to LBB. N.M.D. is a recipient of grants from SPW-EER (convention 1610365, ERA-HDHL cofunded call BioNH 2016) , from the Fonds de la Recherche Scientifique (FRS-FNRS) (PINT-MULTI R.8013.19 (NEURON-ERANET, call 2019) and PDR T.0068.19) and from UCLouvain (Action de Recherche Concertée ARC18-23/092). P.D.C. is recipient of grants WELBIO-CR-2019C-02R and *Funds Baillet Latour* grant for medical research 2015. P. E.P. is supported by AIRC MFAG 21564. The ACTICA study was supported by the Cancer Plan, Belgian Ministry of Public Health (FPS Health), the Belgian Foundation against Cancer and the Saint-Luc Foundation. The funders had no role in study design, data collection and analysis, interpretation of the results, decision to publish, or preparation of the manuscript.

Author contributions

Conception and design of the work were performed by L.B.B. Data collection was caried out by M.M.T., M.S., M.R., S.A.P.,

A.M.N., F.D., P.E.P., and L.B.B. Data analysis and interpretation were performed by M.M.T., M.S., G.G.M., N.M.D., and L.B.B. Help with histological analyses was provided by M.L.R., J.G., and I.A.L. G.D. and J.B.D. provided guidance on RNAseq. Advice on the design was provided by A.T. and S.L. Access to critical equipment was provided by A.E. and P.D.C. A.L. and J.P.T. performed clinical data collection. Funding were acquired by G.G.M., N.M.D., and L.B.B. Drafting the article was performed by M.M.T. and L.B.B. All authors carried out the critical revision of the article. All authors approved the version to be published.

Acknowledgements

We thank Marie Ferrier, Bouazza Es Saadi, Isabelle Blave, Myriam Hsu, and Véronique Allaeys for their skilled technical assistance. We are grateful to Dr Caroline Bouzin and the IREC Imaging Platform (2IP) for their assistance with histological analyses.

Online supplementary material

Additional supporting information may be found online in the Supporting Information section at the end of the article.

Figure S1 Bile acid pathways are altered in cachectic mice. (A) Ileal expression of *Fgf15* by qPCR and **(B)** portal levels of FGF15 by western blot analysis in C26-transplanted mice (C26) as compared to sham-injected mice (CT). *Fgf15*, Fibroblast growth factor 15. N=7-8 mice/group, data are presented as mean ± SEM, *p<0.05, ***p<0.001.

Figure S2 Hematoxylin and eosin-stained liver sections of control (CT) and cachectic mice (C26). Arrows indicate inflammatory cells. Scale of 100 Mm, magnitude 10X.

Figure S3 Progression of the cachectic features and hepatic alterations in cachectic mice. (A) Body weight and food intake evolution, subcutaneous (SAT), brown adipose tissue (BAT) and gastrocnemius (GAS) weight evolution at 8, 9 and 10 days after C26 cell injection (C26) or sham-injected mice (CT). Evolution of gene expression levels involved in muscle atrophy in the gastrocnemius **(B)** and hepatic alterations **(C)** at 8, 9 and 10 days after injection. N=7-8 mice/group, data are presented as mean ± SEM, *p<0.05, **p<0.01, ***p<0.001 vs CT group.

Figure S4 Evolution of bile acid profile in the liver of C26 cachectic mice. (A) Hepatic total bile acid levels and **(B)** bile acid profile in mice at 8, 9 and 10 days after C26 cell injection (C26) or sham-injection (CT). N=7-8 mice/group, data are presented as mean ± SEM, *p<0.05, **p<0.01, ***p<0.001 vs CT group.

Figure S5 Minor effects of cholestyramine treatment on muscle atrophy and thermogenesis in cachectic mice (A) Expression level of *Fgf15* in the ileum of sham-injected mice (CT), in untreated C26-transplanted mice (C26) and in C26-transplanted mice receiving cholestyramine in their diet (C26-CHO). **(B)** Tumor weight in C26 and C26-CHO, as well as food intake evolution of CT, C26 and C26-CHO mice. ***p<0.001 vs CT. **(C)** Body weight evolution and body weight kinetic between day 8 and 10 after cell injection in CT, C26 and C26-CHO mice. (left; ***p<0.001 vs CT) (right; ***p<0.001 vs CT; #p<0.05 and ###p<0.001 vs C26). **(D)** Expression levels of genes involved in muscle atrophy in the gastrocnemius of CT, C26 and C26-CHO mice. **(E)** Expression levels of genes involved in brown adipose tissue thermogenesis in the brown adipose tissue of CT, C26 and C26-CHO mice. *Fgf15*, Fibroblast growth factor 15; *Map1lc3a*, Microtubule Associated Protein 1 Light Chain 3 Alpha; *Trim63*, Tripartite Motif Containing 63 (also known as Murf1); *Fbxo32*, F-Box Protein 32 (also known as Atrogin1); *Ctsl*, Cathepsin L; *Dio2*, iodothyronine deiodinase 2; *Ucp1*, uncoupling protein 1; *Acox1*, Acyl-CoA oxidase 1; *Cidea*, cell death inducing DFFA like effector a; *Gk*, glycerol kinase; *Lpl*, lipoprotein lipase. N=7-8 mice/group, data are presented as mean ± SEM, *p<0.05, **p<0.01, ***p<0.001 vs C26.

Figure S6 Reduced food intake is not the main driver of hepatic alterations in cachectic mice. (A) mRNA expression of genes involved in bile acid metabolism and inflammation in the liver. **(B)** mRNA expression of *Fgf15* in the ileum. Mice were either sham-injected (CT), transplanted with cancer cells (C26), sham-injected and pair-fed to CT mice (CT-PF) or sham-injected and pair-fed to C26 mice (C26-PF). *Cyp7b1*, cytochrome P450 family 7 subfamily B member 1; *Cyp8b1*, cytochrome P450 family 8 subfamily B member 1; *Ntcp*, Na (+)/taurocholate transport protein; *Bsep*, Bile Salt Export Pump; *Cxcl2*, C-X-C motif chemokine ligand 2; *Icam1*, intercellular adhesion molecule 1;*Fgf15*, Fibroblast growth factor 15. N=7-8 mice/group, data are presented as mean ± SEM, *p<0.05, **p<0.01, ***p<0.001.

Data S1. Supporting Information

Table S1 Supporting Information

Table S2 Supporting Information

Table S3 Supporting Information

Table S4 Supporting Information

Table S5 Colorectal cancer patients and tumour characteristics

Conflict of interest

The authors declare that the research was conducted in the absence of any commercial or financial relationships that could be construed as a potential conflict of interest.

Ethical approval

Mouse and human experiments were performed in accordance with local and national ethical regulations. All authors of this manuscript comply with the guidelines of ethical authorship and publishing in the *Journal of Cachexia, Sarcopenia and Muscle*.[72]

References

1. Argiles, J.M., Stemmler, B., Lopez-Soriano, F.J. and Busquets, S. (2018) 'Inter-tissue communication in cancer cachexia'. *Nature Reviews. Endocrinology*, Vol. **15**, pp. 9–20.
2. Baracos, V.E., Martin, L., Korc, M., Guttridge, D.C. and Fearon, K.C. (2018) 'Cancer-associated cachexia'. *Nature Reviews. Disease Primers*, Vol. **4**, 17105.
3. Fearon, K., Strasser, F., Anker, S.D., Bosaeus, I., Bruera, E., Fainsinger, R.L. *et al*. (2011) 'Definition and classification of cancer cachexia: an international consensus'. *The Lancet Oncology*, Vol. **12**, pp. 489–495.
4. Petruzzelli, M., Schweiger, M., Schreiber, R., Campos-Olivas, R., Tsoli, M., Allen, J. *et al*. (2014) 'A switch from white to brown fat increases energy expenditure in cancer-associated cachexia'. *Cell Metabolism*, Vol. **20**, pp. 433–447.
5. Farkas, J., von Haehling, S., Kalantar-Zadeh, K., Morley, J.E., Anker, S.D. and Lainscak, M. (2013) 'Cachexia as a major public health problem: frequent, costly, and deadly'. *Journal of Cachexia, Sarcopenia and Muscle*, Vol. **4**, pp. 173–178.
6. Schmidt, S.F., Rohm, M., Herzig, S. and Berriel Diaz, M. (2018) 'Cancer Cachexia: More Than Skeletal Muscle Wasting'. *Trends Cancer*, Vol. **4**, pp. 849–860.
7. von Haehling, S., Anker, M.S. and Anker, S. D. (2016) 'Prevalence and clinical impact of cachexia in chronic illness in Europe, USA, and Japan: facts and numbers update 2016'. *Journal of Cachexia, Sarcopenia and Muscle*, Vol. **7**, pp. 507–509.
8. Rohm, M., Zeigerer, A., Machado, J. and Herzig, S. (2019) 'Energy metabolism in cachexia'. *EMBO Reports*, Vol. **20**.
9. Lieffers, J.R., Mourtzakis, M., Hall, K.D., McCargar, L.J. and Prado, C.M. (2009) 'Baracos VE. A viscerally driven cachexia syndrome in patients with advanced colorectal cancer: contributions of organ and tumor mass to whole-body energy demands'. *The American Journal of Clinical Nutrition*, Vol. **89**, pp. 1173–1179.
10. Friesen, D.E., Baracos, V.E. and Tuszynski, J. A. (2015) 'Modeling the energetic cost of cancer as a result of altered energy metabolism: implications for cachexia'. *Theore Bio Med Mod*, Vol. **12**, 17.
11. Falconer, J.S., Fearon, K.C., Plester, C.E., Ross, J.A. and Carter, D.C. (1994) 'Cytokines, the acute-phase response, and resting energy expenditure in cachectic patients with pancreatic cancer'. *Annals of Surgery*, Vol. **219**, pp. 325–331.
12. Fearon, K.C., Barber, M.D., Falconer, J.S., McMillan, D.C., Ross, J.A. and Preston, T. (1999) 'Pancreatic cancer as a model: inflammatory mediators, acute-phase response, and cancer cachexia'. *World Journal of Surgery*, Vol. **23**, pp. 584–588.
13. Julienne, C.M., Tardieu, M., Chevalier, S., Pinault, M., Bougnoux, P., Labarthe, F. *et al*. (2014) 'Cardiolipin content is involved in liver mitochondrial energy wasting associated with cancer-induced cachexia without the involvement of adenine nucleotide translocase'. *Biochimica et Biophysica Acta*, Vol. **1842**, pp. 726–733.
14. Halle, J.L., Pena, G.S., Paez, H.G., Castro, A. J., Rossiter, H.B., Visavadiya, N.P. *et al*. (2019) 'Tissue-specific dysregulation of mitochondrial respiratory capacity and coupling control in colon-26 tumor-induced cachexia'. *American Journal of Physiology. Regulatory, Integrative and Comparative Physiology*, Vol. **317**, pp. R68–r82.
15. Khamoui, A.V., Tokmina-Roszyk, D., Rossiter, H.B., Fields, G.B. and Visavadiya, N.P. (2020) 'Hepatic proteome analysis reveals altered mitochondrial metabolism and suppressed acyl-CoA synthetase-1 in colon-26 tumor-induced cachexia'. *Physiological Genomics*.
16. Berriel Diaz, M., Krones-Herzig, A., Metzger, D., Ziegler, A., Vegiopoulos, A., Klingenspor, M. *et al*. (2008) 'Nuclear receptor cofactor receptor interacting protein 140 controls hepatic triglyceride metabolism during wasting in mice'. *Hepatology*, Vol. **48**, pp. 782–791.
17. Jones, A., Friedrich, K., Rohm, M., Schafer, M., Algire, C., Kulozik, P. *et al*. (2013) 'TSC22D4 is a molecular output of hepatic wasting metabolism'. *EMBO Molecular Medicine*, Vol. **5**, pp. 294–308.
18. Rosa-Caldwell, M.E., Brown, J.L., Lee, D.E., Wiggs, M.P., Perry, R.A., Jr., Haynie, W.S. *et al*. (2019) 'Hepatic alterations during the development and progression of cancer cachexia'. *Applied Physiology, Nutrition, and Metabolism*.
19. Tsoli, M. and Robertson, G. (2013) 'Cancer cachexia: malignant inflammation, tumorkines, and metabolic mayhem'. *Trends in Endocrinology and Metabolism*, Vol. **24**, pp. 174–183.
20. Zimmers, T.A., Fishel, M.L. and Bonetto, A. (2016) 'STAT3 in the systemic inflammation of cancer cachexia'. *Seminars in Cell & Developmental Biology*, Vol. **54**, pp. 28–41.
21. Trauner, M., Fickert, P. and Stauber, R.E. (1999) 'Inflammation-induced cholestasis'. *Journal of Gastroenterology and Hepatology*, Vol. **14**, pp. 946–959.
22. Kosters, A. and Karpen, S.J. (2010) 'The role of inflammation in cholestasis: clinical and basic aspects'. *Seminars in Liver Disease*, Vol. **30**, pp. 186–194.
23. Moseley, R.H. (2004) 'Sepsis and cholestasis'. *Clinics in Liver Disease*, Vol. **8**, pp. 83–94.
24. Mulder, J., Karpen, S.J., Tietge, U.J. and Kuipers, F. (2009) 'Nuclear receptors: mediators and modifiers of inflammation-induced cholestasis'. *Front Biosci(Landmark Ed)*, Vol. **14**, pp. 2599–2630.
25. Wagner, M., Zollner, G. and Trauner, M. (2010) 'Nuclear receptor regulation of the adaptive response of bile acid transporters in cholestasis'. *Seminars in Liver Disease*, Vol. **30**, pp. 160–177.
26. Bolder, U., Ton-Nu, H.T., Schteingart, C.D., Frick, E. and Hofmann, A.F. (1997) 'Hepatocyte transport of bile acids and organic anions in endotoxemic rats: impaired uptake and secretion'. *Gastroenterology*, Vol. **112**, pp. 214–225.
27. Woolbright, B.L. and Jaeschke, H. (2016) 'Therapeutic targets for cholestatic liver injury'. *Expert Opinion on Therapeutic Targets*, Vol. **20**, pp. 463–475.
28. Allen, K., Jaeschke, H. and Copple, B.L. (2011) 'Bile acids induce inflammatory genes in hepatocytes: a novel mechanism of inflammation during obstructive cholestasis'. *The American Journal of Pathology*, Vol. **178**, pp. 175–186.
29. Cai, S.Y., Ouyang, X., Chen, Y., Soroka, C.J., Wang, J., Mennone, A. *et al*. (2017) 'Bile acids initiate cholestatic liver injury by triggering a hepatocyte-specific inflammatory response'. *JCI Insight*, Vol. **2**, e90780.
30. Zarrabi, K., Masic, S., Schaefer, C., Bartel, M.J., Kutikov, A. and Zibelman, M. (2020) 'Neoadjuvant checkpoint inhibition in renal cell carcinoma associated Stauffer's syndrome'. *Urol Case Rep*, Vol. **29**, 101077.
31. Koruk, M., Buyukberber, M., Savas, C. and Kadayifci, A. (2004) 'Paraneoplastic cholestasis associated with prostate carcinoma'. *The Turkish Journal of Gastroenterology*, Vol. **15**, pp. 53–55.
32. Barta, S.K., Yahalom, J., Shia, J. and Hamlin, P.A. (2006) 'Idiopathic cholestasis as a

paraneoplastic phenomenon in Hodgkin's lymphoma'. *Clinical Lymphoma & Myeloma*, Vol. **7**, pp. 77–82.
33. Tschirner, A., von Haehling, S., Palus, S., Doehner, W., Anker, S.D. and Springer, J. (2012) 'Ursodeoxycholic acid treatment in a rat model of cancer cachexia'. *Journal of Cachexia, Sarcopenia and Muscle*, Vol. **3**, pp. 31–36.
34. Guillemot-Legris, O., Mutemberezi, V., Cani, P.D. and Muccioli, G.G. (2016) 'Obesity is associated with changes in oxysterol metabolism and levels in mice liver, hypothalamus, adipose tissue and plasma'. *Scientific Reports*, Vol. **6**, 19694.
35. Bessey, O.A., Lowry, O.H. and Brock, M.J. (1946) 'A method for the rapid determination of alkaline phosphates with five cubic millimeters of serum'. *The Journal of Biological Chemistry*, Vol. **164**, pp. 321–329.
36. Loumaye, A., de Barsy, M., Nachit, M., Lause, P., Frateur, L., van Maanen, A. *et al*. (2015) 'Role of Activin A and myostatin in human cancer cachexia'. *Journal of Clinical Endocrinology and Metabolism*, Vol. **100**, pp. 2030–2038.
37. Loumaye, A., de Barsy, M., Nachit, M., Lause, P., van Maanen, A., Trefois, P. *et al*. (2017) 'Circulating Activin A predicts survival in cancer patients'. *Journal of Cachexia, Sarcopenia and Muscle*, Vol. **8**, pp. 768–777.
38. Bonetto, A., Rupert, J.E., Barreto, R. and Zimmers, T.A. (2016) 'The colon-26 carcinoma tumor-bearing mouse as a model for the study of cancer cachexia'. *J visual expers: JoVE*, e54893.
39. Tolson, A.H. and Wang, H. (2010) 'Regulation of drug-metabolizing enzymes by xenobiotic receptors: PXR and CAR'. *Advanced Drug Delivery Reviews*, Vol. **62**, pp. 1238–1249.
40. Cvan Trobec, K., Kerec Kos, M., Trontelj, J., Grabnar, I., Tschirner, A., Palus, S. *et al*. (2015) 'Influence of cancer cachexia on drug liver metabolism and renal elimination in rats'. *Journal of Cachexia, Sarcopenia and Muscle*, Vol. **6**, pp. 45–52.
41. Abrigo, J., Gonzalez, F., Aguirre, F., Tacchi, F., Gonzalez, A., Meza, M.P. *et al*. (2020) 'Cholic acid and deoxycholic acid induce skeletal muscle atrophy through a mechanism dependent on TGR5 receptor'. *Journal of Cellular Physiology*.
42. Watanabe, M., Houten, S.M., Mataki, C., Christoffolete, M.A., Kim, B.W., Sato, H. *et al*. (2006) 'Bile acids induce energy expenditure by promoting intracellular thyroid hormone activation'. *Nature*, Vol. **439**, p. 484.
43. Zhang, L., Voskuijl, W., Mouzaki, M., Groen, A.K., Alexander, J., Bourdon, C. *et al*. (2016) 'Impaired Bile Acid Homeostasis in Children with Severe Acute Malnutrition'. *PLoS ONE*, Vol. **11**, e0155143.
44. Chen, J.L., Walton, K.L., Qian, H., Colgan, T. D., Hagg, A., Watt, M.J. *et al*. (2016) 'Differential Effects of IL6 and Activin A in the Development of Cancer-Associated Cachexia'. *Cancer Research*, Vol. **76**, pp. 5372–5382.
45. Fearon, K.C., Glass, D.J. and Guttridge, D.C. (2012) 'Cancer cachexia: mediators, signaling, and metabolic pathways'. *Cell Metabolism*, Vol. **16**, pp. 153–166.
46. Bindels, L.B., Neyrinck, A.M., Loumaye, A., Catry, E., Walgrave, H., Cherbuy, C. *et al*. (2018) 'Increased gut permeability in cancer cachexia: mechanisms and clinical relevance'. *Oncotarget*, Vol. **9**, 18224.
47. Li, T., Jahan, A. and Chiang, J.Y. (2006) 'Bile acids and cytokines inhibit the human cholesterol 7 alpha-hydroxylase gene via the JNK/c-jun pathway in human liver cells'. *Hepatology*, Vol. **43**, pp. 1202–1210.
48. Gray, S. and Axelsson, B. (2018) 'The prevalence of deranged C-reactive protein and albumin in patients with incurable cancer approaching death'. *PLoS ONE*, Vol. **13**, e0193693.
49. Geier, A., Dietrich, C.G., Voigt, S., Kim, S.K., Gerloff, T., Kullak-Ublick, G.A. *et al*. (2003) 'Effects of proinflammatory cytokines on rat organic anion transporters during toxic liver injury and cholestasis'. *Hepatology*, Vol. **38**, pp. 345–354.
50. Hartmann, G., Cheung, A.K. and Piquette-Miller, M. (2002) 'Inflammatory cytokines, but not bile acids, regulate expression of murine hepatic anion transporters in endotoxemia'. *The Journal of Pharmacology and Experimental Therapeutics*, Vol. **303**, pp. 273–281.
51. Siewert, E., Dietrich, C.G., Lammert, F., Heinrich, P.C., Matern, S., Gartung, C. *et al*. (2004) 'Interleukin-6 regulates hepatic transporters during acute-phase response'. *Biochemical and Biophysical Research Communications*, Vol. **322**, pp. 232–238.
52. Beigneux, A.P., Moser, A.H., Shigenaga, J. K., Grunfeld, C. and Feingold, K.R. (2000) 'The acute phase response is associated with retinoid X receptor repression in rodent liver'. *The Journal of Biological Chemistry*, Vol. **275**, pp. 16390–16399.
53. Wang, B., Cai, S.R., Gao, C., Sladek, F.M. and Ponder, K.P. (2001) 'Lipopolysaccharide results in a marked decrease in hepatocyte nuclear factor 4 alpha in rat liver'. *Hepatology*, Vol. **34**, pp. 979–989.
54. Denson, L.A., Auld, K.L., Schiek, D.S., McClure, M.H., Mangelsdorf, D.J. and Karpen, S.J. (2000) 'Interleukin-1beta suppresses retinoid transactivation of two hepatic transporter genes involved in bile formation'. *The Journal of Biological Chemistry*, Vol. **275**, pp. 8835–8843.
55. Beigneux, A.P., Moser, A.H., Shigenaga, J. K., Grunfeld, C. and Feingold, K.R. (2002) 'Reduction in cytochrome P-450 enzyme expression is associated with repression of CAR (constitutive androstane receptor) and PXR (pregnane X receptor) in mouse liver during the acute phase response'. *Biochemical and Biophysical Research Communications*, Vol. **293**, pp. 145–149.
56. Stedman, C.A., Liddle, C., Coulter, S.A., Sonoda, J., Alvarez, J.G., Moore, D.D. *et al*. (2005) 'Nuclear receptors constitutive androstane receptor and pregnane X receptor ameliorate cholestatic liver injury'. *Proceedings of the National Academy of Sciences of the United States of America*, Vol. **102**, pp. 2063–2068.
57. Gabbia, D., Pozzo, L., Zigiotto, G., Roverso, M., Sacchi, D., Dalla Pozza, A. *et al*. (2018) 'Dexamethasone counteracts hepatic inflammation and oxidative stress in cholestatic rats via CAR activation'. *PLoS ONE*, Vol. **13**, e0204336.
58. Sjoberg, B.G., Straniero, S., Angelin, B. and Rudling, M. (2017) 'Cholestyramine treatment of healthy humans rapidly induces transient hypertriglyceridemia when treatment is initiated'. *American Journal of Physiology. Endocrinology and Metabolism*, Vol. **313**, pp. E167–e74.
59. Out, C., Hageman, J., Bloks, V.W., Gerrits, H., Sollewijn Gelpke, M.D., Bos, T. *et al*. (2011) 'Liver receptor homolog-1 is critical for adequate up-regulation of Cyp7a1 gene transcription and bile salt synthesis during bile salt sequestration'. *Hepatology*, Vol. **53**, pp. 2075–2085.
60. Fuchs, C.D., Paumgartner, G., Mlitz, V., Kunczer, V., Halilbasic, E., Leditznig, N. *et al*. (2018) 'Colesevelam attenuates cholestatic liver and bile duct injury in Mdr2 (-/-) mice by modulating composition, signalling and excretion of faecal bile acids'. *Gut*, Vol. **67**, pp. 1683–1691.
61. Jiang, F., Zhang, Z., Zhang, Y., Wu, J., Yu, L. and Liu, S. (2016) 'L-carnitine ameliorates the liver inflammatory response by regulating carnitine palmitoyltransferase I-dependent PPARγ signaling'. *Molecular Medicine Reports*, Vol. **13**, pp. 1320–1328.
62. Seelaender, M.C., Curi, R., Colquhoun, A., Williams, J.F. and Zammitt, V.A. (1998) 'Carnitine palmitoyltransferase II activity is decreased in liver mitochondria of cachectic rats bearing the Walker 256 carcinosarcoma: effect of indomethacin treatment'. *Biochemistry and Molecular Biology International*, Vol. **44**, pp. 185–193.
63. Wang, W., Andersson, M., Lönnroth, C., Svanberg, E. and Lundholm, K. (2005) 'Prostaglandin E and prostacyclin receptor expression in tumor and host tissues from MCG 101-bearing mice: a model with prostanoid-related cachexia'. *International Journal of Cancer*, Vol. **115**, pp. 582–590.
64. Martignoni, M.E., Dimitriu, C., Bachmann, J., Krakowski-Rosen, H., Ketterer, K., Kinscherf, R. *et al*. (2009) 'Liver macrophages contribute to pancreatic cancer-related cachexia'. *Oncology Reports*, Vol. **21**, pp. 363–369.
65. Prokopchuk, O., Steinacker, J.M., Nitsche, U., Otto, S., Bachmann, J., Schubert, E.C. *et al*. (2017) 'IL-4 mRNA Is Downregulated in the Liver of Pancreatic Cancer Patients Suffering from Cachexia'. *Nutrition and Cancer*, Vol. **69**, pp. 84–91.
66. Schwarz, S., Prokopchuk, O., Esefeld, K., Groschel, S., Bachmann, J., Lorenzen, S. *et al*. (2017) 'The clinical picture of cachexia: a mosaic of different parameters (experience of 503 patients)'. *BMC Cancer*, Vol. **17**, p. 130.
67. Bindels, L.B., Neyrinck, A.M., Claus, S.P., Le Roy, C.I., Grangette, C., Pot, B. *et al*. (2016) 'Synbiotic approach restores intestinal homeostasis and prolongs survival in leukaemic mice with cachexia'. *The ISME Journal*, Vol. **10**, p. 1456.

68. Bindels, L.B., Neyrinck, A.M., Salazar, N., Taminiau, B., Druart, C., Muccioli, G.G. *et al*. (2015) 'Non Digestible Oligosaccharides Modulate the Gut Microbiota to Control the Development of Leukemia and Associated Cachexia in Mice'. *PLoS ONE*, Vol. **10**, e0131009.
69. Ebner, N., Anker, S.D. and von Haehling, S. (2019) 'Recent developments in the field of cachexia, sarcopenia, and muscle wasting: highlights from the 11th Cachexia Conference'. *Journal of Cachexia, Sarcopenia and Muscle*, Vol. **10**, pp. 218–225.
70. Ridlon, J.M., Kang, D.J., Hylemon, P.B. and Bajaj, J.S. (2014) 'Bile acids and the gut microbiome'. *Current Opinion in Gastroenterology*, Vol. **30**, pp. 332–338.
71. Wahlström, A., Sayin, S.I., Marschall, H.-U. and Bäckhed, F. (2016) 'Intestinal crosstalk between bile acids and microbiota and its impact on host metabolism'. *Cell Metabolism*, Vol. **24**, pp. 41–50.
72. von Haehling S, Morley JE, Coats AJS, Anker SD. Ethical guidelines for publishing in the Journal of Cachexia, Sarcopenia and Muscle: update 2019. *J Cachexia Sarcopenia Muscle* 2019;**10**:1143–1145.